平成 27 年度　学位論文

TDP-43 凝集機構に関する研究　(英文)

首都大学東京大学院

理工学研究科　生命科学専攻

学習番号　13981305

下中　翔太郎

指導教官　久永　眞市　教授

(東京都医学総合研究所　長谷川　成人　客員教授)

Contents

Abstract

TAR DNA-binding protein of 43 kDa (TDP-43) has been identified as the major component of ubiquitin-positive neuronal and glial inclusions in frontotemporal lobar degeneration (FTLD) and amyotrophic lateral sclerosis (ALS). Aggregation of TDP-43 to amyloid-like fibrils and spreading of the aggregates are suggested to account for the pathogenesis and progression of these diseases. To investigate the molecular mechanisms of TDP-43 aggregation I attempted to identify the amino acid sequence required for the aggregation. By expressing a series of deletion mutants lacking 20 amino acid residues in the carboxyl-terminal region in SH-SY5Y cells, I established that residues 274-313 in the glycine-rich region are essential for aggregation. *In vitro* aggregation experiments using synthetic peptides of 40 amino acids from this sequence and adjacent regions showed that peptides 274-313 and 314-353 formed amyloid-like fibrils. Transduction of these fibrils induced seed-dependent aggregation of TDP-43 in cells expressing wild-type TDP-43 or TDP-43 lacking nuclear localization signal. These cells showed different phosphorylated C-terminal fragments of TDP-43 and different trypsin-resistant bands. These results suggest that residues 274-353 are responsible for the conversion of TDP-43 to amyloid-like fibrils, and that templated aggregation of TDP-43 by seeding with different peptides induces various types of TDP-43 pathologies, i.e., the peptides appear to act like prion strains.

Introduction

Frontotemporal lobar degeneration (FTLD) is the second most common dementing disorder in patients under 65 years of age, and is characterized by progressive atrophy of the frontal and temporal lobes in the brain. Amyotrophic lateral sclerosis (ALS) is a fatal neurodegenerative disease characterized by progressive motor neuron degeneration. In 2006, TAR DNA-binding protein of 43 kDa (TDP-43) was identified as the major component of tau-negative, ubiquitin-positive inclusions in these diseases (1, 2) (Intro.1). TDP-43 is a heterogeneous nuclear ribonucleoprotein of 414 amino acids, originally identified as a transcriptional repressor that binds to the transactivation responsive region of HIV-1 gene (3). It is expressed ubiquitously and is localized mainly in nuclei, functioning in exon splicing, gene transcription, regulation of mRNA stability and biosynthesis, and the formation of nuclear bodies. For example, it has been reported that TDP-43 binds to the junctional region between exons 9 and 10 of the gene coding cystic fibrosis transmembrane conductance regulator (CFTR) and causes skipping of exon 9 (4). Structurally, TDP-43 is characterized by two RNA-recognition motifs, a C-terminal tail that contains a glycine-rich region, and a glutamine/asparagine (Q/N)-rich region.

Discovery of missense mutations in the *TARBDP* gene in patients with familial and sporadic ALS and FTLD (5-12) demonstrated a direct link between genetic lesion and development of TDP-43 pathology. Importantly, most of the mutations are localized in the carboxy-third of the molecule, which

shows sequence similarity to prion proteins (Intro. 2). Furthermore, biochemical and histological analyses demonstrated accumulation of full-length and carboxy-terminal fragments (CTFs) in hyperphosphorylated and fibrillar forms in brain and spinal cord of patients (13). Furthermore, the CTFs banding patterns are different between the diseases, and are closely related to the neuropathological phenotypes, which can be classified into at least three groups (types A~C) (13, 14). The CTFs banding patterns are considered to reflect the protease resistance of the assembled protein structures (15). It was recently demonstrated that the pathological TDP-43 has prion-like activity, and can convert normal TDP-43 to an abnormal form in cultured cells (16) (Intro. 3). Interestingly, the CTFs banding patterns of converted host proteins resemble those of the pathological TDP-43 used as seeds, suggesting that the conversion is template-dependent.

These findings strongly suggest that aggregation of C-terminal regions of TDP-43 plays a central role in the pathogenesis and progression of ALS and FTLD with ubiquitin positive inclusions (FTLD-U). The aggregation of CTFs of TDP-43 has also been demonstrated in experimental cellular models; for example, our previous study showed that expression of CTF (162-414) of TDP-43 with a GFP-tag in SH-SY5Y cells induced cytosolic mislocalization of TDP-43 in phosphorylated and ubiquitinated aggregates, recapitulating the TDP-43 pathology in brains (17).

In this study, I investigated aggregation of TDP-43 in cultured cells expressing a series of deletion constructs in order to identify the sequences responsible for the aggregation. Then, self-aggregation of

synthetic peptides derived from the identified sequence and surrounding sequences was examined. Synthetic fibrillar aggregates of peptides from the identified sequence were found to work as seeds, converting normal TDP-43 into abnormal aggregates in cultured cells.

Materiuals and Methods

Construction of plasmids

To construct a series of deletion mutants lacking sequences of 20 amino acid residues in TDP-CTF with a GFP tag, I conducted site-directed mutagenesis of pEGFP–TDP (162-414) (17). PCR was carried out using a site-directed mutagenesis kit (Strategene) with the following primers: for Del1 (lacking 214-233), forward, 5'- GAGTTCTTCTCTCAGTTTGCAGATGATCAG-3', and reverse, 5'-CTGATCATCTGCAAACTGAGA GAAGAACTC-3', for Del 2 (lacking 234-253), forward, 5'-TTTGCCTTTGTTACAAGCGTTCATA TATCC-3', and reverse, 5'-GGATATATGAACGC TTGTAACAAAGGCAAA-3', for Del 3 (lacking 254-273), forward, 5'-ATCATTAAAGGAATCGGA AGATTTGGTGGT-3', and reverse, 5'-ACCACCAA ATCTTCCGATTCCTTTAATGAT-3', for Del 4 (lacking 274-293), forward 5'-CAGTTAGAAAGA AGTGGGGGTGGAGCTGGT-3', and reverse, 5'-ACCAGCTCCACCCCCACTTCTTTCTAACTG-3', for Del 5 (lacking 294-313), forward, 5'-TTTGG TAATAGCAGAGGTGCGTTCAGCATT-3', reverse, 5'-AATGCTGAACGCACCTCTGCTATTACCAA-3', for Del 6 (lacking 314-333), forward, 5'-GGTGGGATGAACTTTTGGGGTATGATGGGC-3', and reverse, 5'-GCCCATCATACCCCAAA AGTTCATCCCACC-3', for Del 7 (lacking 334-353), forward,

5’-GCACTACAGAGCAGTCAAAACCAA GGCAAC-3’, and reverse, 5’-GTTGCCTTGGTTT TGACTGCTCTGTAGTGC-3’, for Del 8 (lacking 354-373), forward, ’-CCATCGGGTAATAACTATA GTGGCTCTAAT-3’, and reverse, 5’-ATTAGAGC CACTATAGTTATTACCCGATGG-3’, for Del 9 (lacking 374-393), forward, 5’-TCTGGAAATAAC TCTGGCAGTGGTTTTAAT-3’, and reverse, 5’-AT TAAAACCACTGCCAGAGTTATTTCCAGA-3’. Deletion mutants lacking 40 amino acid residues were also constructed from GFP-tagged TDP-CTF (162-414), full-length TDP-43 and TDP-43 (ΔNLS &187-192). Twenty amino acid length deletions of Del 2, 4 and 5 were induced in pEGFP–TDP (162-414), pcDNA3-TDP-43 and pcDNA3-TDP-43 (ΔNLS &187-192) (18) as described above and PCR was conducted with the following primers: For Del (234-273), Del 2 (234-253) was used as a template and primers were forward, 5’-TTTGCCTTTGTTAC AGGAAGATTTGGTGGT-3’, and reverse, 5`-ACCA CCAAATCTTCCTGTAACAAAGGCAAA -3’, For Del (274-313), Del 4 (274-293) was used as a template and primers were forward, 5’-CAGTTAGAAAGA AGTGGTGCGTTCAGCATT-3’, and reverse, 5`-AA TGCTGAACGCACCACTTCTTTCTAACTG-3’, For Del (314-353), Del 6 (314-333) was used as a template and primers were forward, 5’- GGTGG GATGAACTTTCAAAACCAAGGCAAC-3’, and reverse, 5`-GTTGCCTTGGTTTTGAAAGTTCATC CCACC-3’. All gene recombination experiments were approved by the Committee for Safe Handling of Living Modified Organisms and Pathogens of

Tokyo Metropolitan Institute of Medical Science and performed in accordance with the guidelines of the committee.

Antibodies

A monoclonal antibody specific for GFP was purchased from MBL. An antibody specific for TDP-43 (monoclonal and polyclonal) was obtained from Proteintech. Monoclonal and polyclonal antibodies specific for abnormal phosphorylation of TDP-43 (pS409/410), and a polyclonal antibody specific for TDP-43 C-terminal region (405-414) were prepared as previously described (13, 19). As secondary antibodies, biotin-labeled secondary antibody was purchased from Vector for use in the Avidin-Biotin Complex (ABC) method and goat anti-mouse IgG (H+L)-HRP conjugate was obtained from BioRad for use in the enhanced chemiluminescence (ECL) method.

Cell culture and transfection of plasmids

SH-SY5Y cells were cultured in Dulbecco's modified Eagle's medium (DMEM)/F-12 medium (Sigma) supplemented with 10% fetal calf serum, MEM nonessential amino acid solution (Gibco), and penicillin-streptomycin-glutamine (Gibco). Cells were maintained at 37℃ under a humidified atmosphere of 5% CO_2 in a culture chamber. Cells were grown to 50% confluence in six-well culture dishes and transfection of expression plasmids into cells was carried out using

FuGENE6 (Roche) according to the manufacturer`s instructions.

Immunoblot analysis

Transfected SH-SY5Y cells were incubated in six-well plates for the indicated time and harvested in A68 buffer (10 mM Tris-HCl pH 7.5, 10% sucrose, 0.8 M NaCl, 1 mM EGTA) containing 1% sarkosyl (Sar). Cell lysate was centrifuged at 100,000 × g for 20 min at 4℃, and the supernatant was recovered as the Sar-soluble fraction. The remaining pellets were lysed in SDS-sample buffer and heated at 100℃ for 5 min to prepare the Sar-insoluble fraction. Sar-insoluble fraction was also prepared from brains of patients with FTD or ALS as described (13). Trypsin digestion of the Sar-insoluble fraction was performed by incubation in 30 mM Tris-HCl buffer (pH 7.4) containing 0.01 mg/mL trypsin at 37℃ for 30 min. Protein concentration was estimated using BCA Protein Assay Kit (Pierce). Samples were loaded on 12.5 % SDS-PAGE gels electrophoresed with Tris-glycine buffer system. Proteins in gels were transferred onto a polyvinylidene difluoride membrane (Millipore) and blocked with 3% gelatin. The blots were incubated overnight with the indicated primary antibodies in 10% calf serum at an appropriate dilution (1: 1000-5000) at room temperature. Membranes were washed and incubated for 1 h with a biotin-labeled secondary antibody (Vector) or a horseradish peroxidase-labeled secondary antibody (BIO-RAD) at room temperature. Signals were detected using an ABC staining kit (Vector) or ECL Prime Western blotting Detection System (GE Healthcare).

Fluorescence microscopic analysis

SH-SY5Y cells transfected with expression plasmids were grown on 35 mm glass dishes (Iwaki) for 2 days. To observe intracellular aggregates of GFP-tagged TDP-CTF (they show intense fluorescence of GFP), cells were examined with a fluorescence microscope (DIAPHOTO, Nikon) set at 488 nm. Quantitation of aggregates formation was performed as follows: nine images were acquired using a fluorescence microscope (Biozero, KEYENCE), using a sliding field of view. The nine images were combined to form a single image using BZ-2 Analyzer (KEYENCE) and luminance extraction was conducted to quantify the fluorescence of aggregates in the image. The lower limit threshold of luminance for extraction was adjusted to exclude the fluorescence of non-aggregated protein (which is weaker than that of aggregated protein), so that only luminance of aggregated TDP-CTF was detected and quantified.

In vitro aggregation of synthetic peptides

Synthetic 40mer peptides with the following partial sequences of TDP-43 (234-273: FADDQIAQSLCGE DLIIKGISVHISNAEPKHNSNRQLERS, 274-313: GRFGGNPGGFGNQGGFGNSRGGGAGLGNNQGSNMGGGMNF, 314-353: GAFSINPAMMAAAQ AALQSSWGMMGMLASQQNQSGPSGNN, 353- 392:

QNQGNMQREPNQAFGSGNNSYSGSNSGA AIGWGSASNAGS) and Control (NHYVKMILKK ALSRYPNRRNLPCVDLRYKRKSIILQRKYS were dissolved in DMSO and diluted with Tris-HCl (pH 7.5) to the indicated concentrations. These peptide solutions were incubated on a shaker at 37°C, and 10 μL aliquots were added to 300 μL 20 mM MOPS buffer containing 5 μM thioflavin S at the indicated time. After 30 min incubation at room temperature, 200 μL was aliquots were loaded on a 96-well black plate and fluorescence of thioflavin S (λex = 436 nm, λem = 535 nm) was measured using a luminescence plate reader (Chameleon, HIDEX).

Transmission electron microscopy

For electron microscopy, peptide solutions were incubated on a shaker for 8 days, placed on collodion-coated 300-mesh copper grids, and stained with 2% (v/v) phosphotungstate. Micrographs were recorded on a JEOL 1200EX electron microscope.

Induction of TDP-43 aggregation in cells by peptide fibrils

Aliquots of 100 μL TDP-43 peptide solutions were incubated for 8 days on a shaker, diluted with 500 μL 30mM Tris-HCl (pH 7.5) and centrifuged at 100,000 × g for 20 min. After centrifugation, the supernatant was removed and remaining pellets (peptide fibrils) were dissolved in 30 mM Tris-HCl (pH 7.5). Aliquots of 5 μL of peptide fibril solution were added to 95 μL 6 M guanidine

HCl solution and peptide fibrils were quantified by means of HPLC. For introduction into cells, 5 μg of peptide fibrils was mixed with 120 μL opti-MEM and 62.5 μL Multifectam (Promega) was added. After incubation for 30 min at room temperature, 62.5 μL opti-MEM was added. The mixture was further incubated for 5 min, and added to cells immediately after transfection of expression plasmids of TDP-43. The treated cells were further incubated for 2 days in a CO_2 incubator.

Immunocytochemistry

Transfection of expression plasmids and induction of peptide fibrils were conducted as described above, using SH-SY5Y cells grown on coverslips. After incubation for 2 days in a CO_2 incubator, cells were fixed with 4% paraformaldehyde and stained with the indicated primary antibodies at 1:1000 dilution. After incubation for 1 hr, cells were washed and treated with secondary antibodies (Anti-Rabbit IgG-Conjugated Alexa-568, Anti-Mouse IgG-conjugated Alexa-488, Invitrogen) and TO-PRO-3 (Invitrogen) to counterstain nuclear DNA. After 1 hr, the cells were mounted and analyzed using LSM5 Pascal confocal microscope (Carl Zeiss).

Cell death assay

Cell death assays were conducted using a CytoTox 96 Non-Radioactive Cytotoxicity Assay Kit (Promega).

Statistical analysis

All values in figures are mean ± SEM. Biochemical data were statistically analyzed using the unpaired, two-tailed Student's t test. A p value of ≤ 0.05 was considered statistically significant.

Results

Expression and aggregation of deletion mutants lacking 20 amino acids in SH-SY5Y cells.

In order to determine the sequences responsible for aggregation of CTFs of TDP-43, I constructed a series of deletion mutants lacking 20 amino acid residues in TDP-CTF with a GFP tag: Del 1(Δ214-233), Del 2(Δ234-253), Del 3(Δ254-273), Del 4(Δ274-293), Del 5(Δ294-313), Del 6(Δ314-333), Del 7(Δ334-353), Del 8(Δ354-373) and Del 9(Δ374-393) (Fig. 1A and B). Aggregation of TDP-43 in cells transfected with a deletion or wild-type construct was evaluated by biochemical analysis of Sar-insoluble TDP-43 (Fig. 2). The Sar-soluble TDP-43 CTF levels were similar among the deletions as detected with anti-GFP (Fig. 2 left panel), but remarkable decreases of Sar-insoluble TDP-43 were detected with anti-GFP or pS409/410 in cells expressing Del 4, 5 or 8 (Fig. 2 middle and right panels). The results of band quantitation are shown in the lower panels. These data suggest that deletion of residues 274-293, 294-313 or 354-373 reduced the TDP-43 aggregation.

Aggregation of the deletion mutants of TDP-43 was also evaluated by means of fluorescence microscopy (Fig. 3). In cells expressing Del 1, 2 or 3, many small dot-like aggregates were observed, which were morphologically distinct from those in cells expressing wild-type CTF. In contrast, only small amounts of TDP-43 aggregates, or none, were observed in cells expressing Del 4, 5, 6, 7 or 8, compared to those in cells expressing wild-type or Del 9. Intracellular aggregates of GFP-tagged TDP-43 CTF had much more intense fluorescence than diffusely expressed non-aggregated GFP-tagged

TDP-43 CTF. Therefore, to quantify TDP-43 aggregates by luminance extraction, I adjusted the lower limit (threshold) of luminance value so that only the aggregates were detected. As shown in Fig. 3B, markedly reduced aggregate formation was observed in cells expressing Del 4~8, confirming the visual observations. These results indicate that sequences in the region between 274-373 are responsible for the aggregation of TDP-CTF, although there is some discrepancy between the results of these morphological observations and those of biochemical analyses shown in Fig. 2. It is possible that amorphous aggregates, which are different from the amyloid-like aggregates, but are nevertheless insoluble and phosphorylated, are formed in cells due to deletion of the sequence 314-353. Such aggregates might be diffusely localized in cytoplasm of cells, and would not be detected as aggregates by fluorescence microscopy.

Expression and aggregation of deletion mutants lacking 40 amino acids in SH-SY5Y cells.

To further analyze the effect of these sequences on TDP-43 aggregation, I constructed another series of deletion mutants lacking 40 amino acid residues in GFP-tagged TDP-CTF and an untagged full-length TDP-43 mutant (ΔNLS &187-192) which lacks both the nuclear localization signal (NLS: 78-84) and a similar sequence (187-192), and forms aggregates in cells (18). Remarkable reduction of aggregation was observed both biochemically and morphologically in cells expressing the Del 4 and Del 5 mutants described above. The sequences deleted in these mutants correspond to the glycine-rich region of TDP-43. Therefore, 40-amino-acid-deletion constructs were made by deleting Del 4-5, and the

adjacent Del 2-3, Del 6-7 and Del 8-9. They were expressed in cells and aggregate formation was investigated by quantitation of Sar-insoluble TDP-43 (Fig. 4). Deletion of residues 234-273 (Del 2-3) in GFP-CTF caused a significant increase of Sar-insoluble phosphorylated TDP-43. In contrast, insoluble TDP-43 was dramatically reduced by deletion of residues 274-313 (Del 4-5), while no reduction was detected in response to deletion of residues 314-353. Deletion of residues 354-393 (Del 8-9) also showed significant reduction of insoluble TDP-43 on the blot with pS409/410 but not with anti-GFP antibody. Aggregate formation of these deletion mutants was also investigated by means of fluorescence microscopy. In cells expressing undeleted GFP-tagged CTF, Del 2-3(234-273) and Del 8-9(354-393), distinct aggregates were observed, whereas diffuse cytoplasmic localization of GFP was observed in cells expressing Del 4-5 (274-313) or Del 6-7 (314-353). The results of quantitation of aggregates (Fig. 5A and B) suggested that residues 314-353 may also be important for aggregation of TDP-CTF. Similar results were observed in a cellular aggregation model using untagged full-length mutant (ΔNLS &187-192)(Fig. 6), suggesting that residues 274-313 and 354-393 are important for aggregation of not only CTF, but also full-length TDP-43.

In vitro aggregation of synthetic peptides of TDP-43.

Next, I investigated whether or not these 40 amino acids peptides can themselves form amyloid-like fibrillar aggregates. Synthetic peptides corresponding to sequences 234-273, 274-313,

314-353, 353-392 of TDP-43 and a control peptide (Fig. 7) were dissolved in 30 mM Tris-HCl buffer at various concentrations (0.05, 0.1 and 0.2 mM), and incubated at 37 C with shaking. Amyloid-like aggregate formation was analyzed in terms of Thioflavin S (ThS) fluorescence. The peptide 234-273 showed an increase of ThS fluorescence at day 4 at a concentration of 0.2 mM, but no increase was observed even by day 8 at lower concentrations. In contrast, the peptides 274-313 and 314-353 showed markedly increased ThS fluorescence at day 1 at most concentrations studied (Fig. 8). No ThS increase was observed with the peptide 353-392 or the control peptide. The amyloid-like aggregates formed by the above peptides at a concentration of 0.2 mM were negatively stained with phosphotungstate on a grid and observed by electron microscopy. As shown in Fig. 9, short fibrillar aggregates were observed in the peptide 234-273 solution. In contrast, relatively long, straight or twisted fibrils (10-15 nm diameter) were observed in the 274-313 and 314-353 peptide solutions. These results indicate that the TDP-43 peptides 274-313 and 314-353 have a high propensity to form amyloid-like fibrils, while 234-273 and 354-393 peptides have a low propensity.

The synthetic peptide fibrils can serve as a seed to convert intracellular TDP-43 into abnormal aggregates.

Prion-like propagation of intracellular abnormal proteins has been demonstrated in cellular and animal models (16, 20). It has also been shown that the Sar-insoluble TDP-43 fibrils prepared from

brains of patients with ALS/FTLD have prion-like properties and can seed-dependently convert normal TDP-43 to abnormal forms. Therefore, I investigated whether fibrils made of these synthetic peptides have the ability to convert normal TDP-43 into abnormal aggregates. SH-SY5Y cells were transiently transfected with wild-type TDP-43 and then transduced with these peptide monomers or the fibrils (234-273, 274-313 and 314-353), and then Sar-soluble and insoluble TDP-43 was analyzed by immunoblotting (Fig. 10A and B). In cells transduced with the monomeric peptides, no insoluble, phosphorylated TDP-43 was detected (Fig. 10A). In contrast, pS409/410-positive, insoluble TDP-43 of 45 kDa was detected in cells transduced with fibrils of peptide 274-313 or peptide 314-353, suggesting that these synthetic peptide fibrils converted wild-type full-length TDP-43 to abnormal aggregates. I also investigated the effect of phosphorylation on seed-dependent TDP-43 aggregation. Mutant TDP-43 (Ser403/404/409/410Ala), in which the four major phosphorylation sites Ser403, Ser404, Ser409 and Ser410 were substituted by alanine, was expressed in cells, which were treated with peptide fibrils. The amount of insoluble TDP-43 was compared to that in cells expressing wild-type TDP-43 by using anti-TDP-43 and anti-TDP-43 (405-414), since pS409/410 could not be used in this case. Immunoblot analysis showed no differences in aggregation between mutant TDP and WT-TDP (Fig. 11), strongly suggesting that phosphorylation of TDP-43 is not necessary for aggregation of TDP-43, but most likely occurs as a secondary event in seed-dependent TDP-43 aggregation.

To confirm the aggregate formation morphologically, I performed immunocytochemical analyses

of cells expressing WT-TDP-43 or ΔNLS-TDP-43 and treated with these fibrils (Fig. 12 and 13). No phosphorylated and aggregated TDP-43 was seen in cells expressing WT-TDP-43 or ΔNLS-TDP-43 alone. On the other hand, dot-like structures positive for pS409/410 were found in WT-TDP-43 transfected cells treated with synthetic peptide fibrils of 274-313 or 314-353. The inclusions were also positive for anti-TDP-43 antibody, which recognizes the middle region of TDP-43. Most of the inclusions appeared to be localized in cytoplasm, not in nuclei, and this was confirmed by image analysis (Fig 14; representative data for cells transfected with WT-TDP-43 + fibril 274-313 are shown). Interestingly, the nuclear staining of endogenous TDP-43 was lost in the cells with cytoplasmic TDP-43 aggregates, recapitulating an important neuropathological feature of TDP-43 proteinopathy. Together with the immunoblot analyses, these results indicate that full-length WT-TDP-43 expressed in cells became aggregated and phosphorylated after introduction of the synthetic peptide fibrils of 274-313 and 314-353, but not with peptide fibrils of 234-273. More cytoplasmic inclusions of TDP-43, positive for both anti-pS409/410 and anti-TDP-43, were detected in cells expressing ΔNLS-TDP-43 and treated with these peptide fibrils. There were no apparent differences in morphology of the inclusions formed in cells treated with peptide fibrils 274-313 and peptide fibrils 314-353.

Distinct conformational changes are induced by different peptide fibrils.

I further investigated these inclusions biochemically to determine whether there is any

difference between the aggregates induced by the 274-313 fibrils and those induced by the 314-353 fibrils. Immunoblot analyses of the Sar-insoluble fractions of cells transfected with WT-TDP-43 or ΔNLS-TDP-43 showed that full-length TDP-43 with an apparent molecular weight of 45 kDa is accumulated in response to treatment with fibrils of peptide 274-313 or peptide 314-353. In addition to the intensely labeled 45 kDa band, some weak bands were also detected in the upper and lower molecular weight regions with both anti-TDP-43 and pS409/410 antibodies (Fig. 15A). Interestingly, the banding patterns at lower molecular weight were different between the treatments with the 274-313 fibrils and the 314-353 fibrils. This was the case both in cells expressing WT-TDP-43 and in cells expressing ΔNLS-TDP-43. This finding may indicate that the different peptide fibrils converted WT-TDP-43 into conformationally distinct aggregates. The finding that these fibrils converted wild-type full-length TDP-43 to abnormal aggregates is important, and to confirm this observation, I treated the Sar-insoluble fractions of these cells with trypsin and then analyzed the trypsin-resistant fragments by immublotting with pS409/410 (Fig. 15B). It should be noted that trypsin-resistant banding patterns are different between different disease phenotypes and the patterns are useful for biochemical classification of TDP-43 proteinopathy. Upon treatment of the Sar-insoluble fractions with trypsin, the full-length TDP-43 band disappeared and bands of 16~24 kDa appeared in the cases of cells treated with the 273-313 fibrils and the 314-353 fibrils. The banding pattern of the 273-313 fibril-treated cells (several major bands at 18, 19 kDa and ~23 kDa) was different from that of the 314-353 fibril-treated cells (one

major band at 18 kDa and one minor band at 16 kDa). To link these results to the molecular pathogenesis of TDP-43 proteinopathy, I compared the banding patterns of TDP-43 aggregates formed in cultured cells by peptide-fibril introduction to those in brains of patients. TDP-43 proteinopathy is subclassified into at least three types based on the predominant TDP-43-positive structures: type A is mainly seen in FTLD-TDP with *PGRN* mutations, type B corresponds to ALS and FTLD-MND, and type C is a representative feature of sporadic FTLD-TDP with impairment of semantic memory. Each type is characterized biochemically by specific patterns of insoluble TDP-43 CTFs detected with anti-pS409/410 (13, 15). In this study, Sar-insoluble fractions were prepared from brains of typical cases with FTD (type A) and ALS (type B). As shown in Fig 16, the trypsin-resistant bands of insoluble TDP-43 from FTD and ALS were very similar to those in cells treated with 274-313 and 314-353 fibrils, respectively, in terms of both patterns and molecular sizes. These results strongly suggest that extracellular introduction of different TDP-43 peptide fibrils induced formation of different types of intracellular TDP-43 aggregates via seeded conversion of full-length WT-TDP-43 and ΔNLS-TDP-43. I also conducted LDH assay to examine cytotoxicity in cells containing intracellular aggregates following peptide-fibril introduction. No significant increase of LDH was detected in this experiment (Fig. 17), suggesting that toxicity of the aggregates is below the detectable limit in this assay.

Molecular mechanism of seed-dependent aggregation of TDP-43.

To investigate the molecular mechanism of the intracellular aggregation of TDP-43 induced by transduction of the peptide fibrils, I expressed deletion mutants of TDP-43 lacking these 40 amino acid sequences, namely TDP-43 (del234-273), TDP-43 (del274-313) and TDP-43 (del314-353) in cells, and then treated the cells with the peptide fibrils. These deletion mutants were detected at ~40 kDa, with apparently lower molecular weight than WT-TDP-43, in the Sar-soluble fraction (Sup). Expression of WT-TDP-43 or deletion mutant TDP-43 (del274-313) or TDP-43 (del314-353) alone did not afford Sar-insoluble phosphorylated TDP-43 (Fig 18A), but a phosphorylated, insoluble 40 kDa band was detected in cells expressing TDP-43 (del234-273). These results indicate that deletion of residues 234-273 from full-length TDP-43 promoted aggregation, but deletion of the other 40 amino acid sequences did not affect aggregation.

Cells expressing these deletion mutants were treated with peptide fibrils and cultured for another 2~3 days. The Sar-insoluble fractions prepared from these cells were analyzed by immunoblotting with anti-TDP-43 and pS409/410. As shown in Fig. 18B, the Sar-insoluble phosphorylated TDP-43 induced by fibrils (274-313) was dramatically decreased in cells expressing TDP-43 lacking residues 274-313, compared to those in cells expressing WT-TDP-43 or the other deletion mutants. Similarly, the Sar-insoluble phosphorylated TDP-43 induced by the fibrils (314-353) was markedly decreased in cells expressing TDP-43 lacking residues 314-353, compared to those in cells expressing WT-TDP-43 or the

other deletion mutants (Fig. 18C). Expression levels of WT and deletion mutants were almost the same as observed in immunoblot analysis of the soluble fractions (Fig. 18B and C). The greater accumulation of insoluble TDP-43 in cells expressing TDP-43 (del 234-237) is probably due to its high propensity to form aggregates (Fig. 18A). Thus, these results demonstrate that seed-dependent conversion of intracellular TDP-43 into abnormal aggregates requires association of fibril seeds with the same sequence in the host protein.

DISCUSSION

In this study, I have identified the region between residues 274-373 of TDP-43 as an essential sequence for aggregation of GFP-tagged TDP-CTF and untagged full-length TDP-43 lacking NLS, as well as the similar (ΔNLS &187-192), by using two series of deletion mutants lacking 20 or 40 amino acids. In addition, synthetic peptides corresponding to residues 274-313 and 314-353 in this region have a high propensity to form amyloid-like fibrils.

The TDP-43 C-terminal domain (233-414) has a moderate level of sequence similarity to prion protein (21), and the two highly amyloidogenic 40 amino acid sequences (274-313 and 314-353) identified in this study cover ~ 44% of this region. The former sequence 274-313 contains 17 Gly residues in the 40 amino acids, corresponding to the glycine-rich region of TDP-43, and 18 amino acids (17 Gly and 1 Asn) are identical and 7 amino acids are similar to those in prion protein. The latter sequence 314-353 contains 9 Gln/Asn and 5 Met residues, covering half of the Q/N rich-region of TDP-43. Within this sequence, 10 amino acids (4 Ala, 2 Gly, 2 Met, 1 Asn, 1 Leu and 1 Ser) are identical and 4 amino acids are similar to those of prion protein (Fig. 19). Reported pathogenic mutations of ALS/FTLD are intensely focused in these regions, and it has been suggested that the A315T mutation increases the tendency of the protein to form beta-sheet structure. Since these two synthetic 40 amino acid peptides have high propensity to form amyloid-like fibrils at low concentration, these sequences are likely to be important for aggregation of full-length TDP-43. In fact, deletion of these sequences resulted

in a dramatic decrease in the formation of dot-like intracellular inclusions in cells expressing GFP-tagged TDP-CTF or untagged full-length TDP-43 (ΔNLS &187-192), although the Sar-insoluble, phosphorylated TDP-43 was not reduced by deleting the sequence of 314-353.

It remains unknown why such inconsistent results were obtained between the biochemical analysis and the observations by fluorescence microscopy. One possible explanation is that the sequence 314-353 may stabilize the TDP-43 molecule, and the deletion leads to formation of amorphous aggregates of oligomers, which are insoluble and phosphorylated, and are diffusely localized in cytoplasm; such structures would not be detected as aggregates by fluorescence microscopy. It remains to be clarified whether such diffusely accumulated TDP-43 has any toxic effect on cells and whether it has any prion-like ability to serve as a seed for TDP-43 aggregation.

The significance of the abnormal phosphorylation in these intracellular abnormal proteins in relation to neurodegenerative diseases has been debated. Our present results clearly show that phosphorylation on Ser403, Ser404, Ser409 and Ser410 has no effect on seed-dependent aggregation of TDP-43, suggesting that phosphorylation may be a secondary event occurring after seed-dependent amyloid-like fibril formation. This may also be the case in other intracellular abnormal amyloid-like protein diseases.

Some research to identify aggregation-related sequences of TDP-43 has been reported. For example, Hu et al. assayed the aggregation ability of a series of N- or C-terminally truncated TDP-43

(C-terminally GFP-tagged form) in an E. coli overexpression system, and proposed that 318-343 is essential for aggregation of TDP-43 (22). A synthetic peptide corresponding to this sequence underwent structural transformation from alpha-helix to beta-sheet during aggregation (22). Wang et al. proposed that the truncated RRM2 (tRRM2: 208-265) has a more important role than the glycine-rich region in TDP-43 aggregation, based on findings in Neuro2A cells overexpressing C-terminally GFP-tagged tRRM-2 or glycine-rich region (23). Saini et al. identified 246-255 and 311-320 as core aggregation sequences of TDP-43 by evaluating the aggregation ability of a series of peptides derived from the TDP-43 C-terminal sequence (220-414) (24). Furukawa et al. reported that the C-terminal half of TDP-43 (i.e. TDP-432-C) can recapitulate the aggregation propensities of the full-length protein (25). Huang's group showed that peptides in the sequence (287-322) have a propensity for aggregation, and this tendency was altered by substitution of glycines with prolines (26, 27). The sequences reported in previous studies and identified in this study are summarized in Fig. 20. Our sequence 274-353 overlaps well with those reported by Huang's group, though other sequences were not identified in this study. The discrepancy may be due to the difference in the length of peptides used in in vitro aggregate formation assay (I prepared 40mers in contrast with their short 8-12mer peptides). Furthermore, I clearly demonstrated the seeding ability of our peptide fibrils, which had not been addressed previously.

Emerging evidence suggests prion-like propagation or spreading of intracellular pathological proteins, including tau, alpha-synuclein and TDP-43, in diseased brains. In fact, the inclusions in brains

of patients are positive for thioflavin S fluorescence and most of these pathological proteins are accumulated in filamentous or fibrous forms. In addition, the paired helical filaments prepared from AD brains and alpha-synuclein fibrils made of recombinant protein were demonstrated to have a cross-beta structure (28, 29), which is the same as that of abnormal prion protein. Furthermore, the seed-dependent prion-like conversion of normal proteins into an abnormal form has been demonstrated experimentally in cellular and animal models (16, 20, 28, 30).

TDP-43 pathologies can be seen in various diseases and are thought to be the cause of neurodegeneration in these diseases, including ALS, FTLD and related disorders, which are referred to as TDP-43 proteinopathy. Clinicopathologically, these TDP-43 proteinopathy can be classified to at least four subtypes (types A-D), and there is a close relation between the pathological subtypes of TDP-43 proteinopathy and the immunoblot patterns of C-terminal fragments of phosphorylated TDP-43 (13, 14, 15). Furthermore, protease-resistant banding patterns of pathological insoluble TDP-43 are also useful for biochemical classification of the subtypes. However, the molecular mechanisms have been unclear. In this study, I demonstrated that fibrils made of synthetic peptides corresponding to the critical regions of TDP-43 have the ability to convert intracellular wild-type TDP-43 into abnormal aggregates, when they are introduced into cells. The TDP-43 aggregates induced by different peptide fibrils showed different CTF banding patterns and different trypsin-resistant bands, strongly suggesting that different seeds induce assembly of TDP-43 into distinct amyloid-like fibrils. I also demonstrated that the

interaction of the seeds with the same peptide sequence in the host protein is required for the seeded aggregation. The distinct seeds formed by assembly of different parts of the C-terminal regions of TDP-43 may convert normal TDP-43 into corresponding abnormal conformations, and thus determine the clinicopathological subtypes of TDP-43 proteinopathy. Cell-to-cell spreading of a single species of pathological protein in brain may account for the relatively homogeneous pathology in individual brains, despite the fact that various types of conformational change or structural assembly can occur.

The sequences identified in this study and the seeded aggregation model that I have developed should be useful for establishing animal models of TDP-43 proteinopathy. The results obtained in this study may also contribute to our understanding of the pathogenesis and progression of TDP-43 proteinopathy.

FIGURE LEGENDS

Intro. 1. TDP-43 in ubiquitin-positive inclusions in ALS and FTLD.

(A) A schematic representation of TDP-43 (RRM: RNA recognition motif, NLS: nuclear localization signal, Gly-rich: glycine-rich domain, Q/N-rich: glutamine/ asparagine- rich domain). (B) An immunostainings of the spinal code in ALS (right) and hippocampal region of FTLD-MND (left) with an anti-ubiquitin antibody (Arai et al., 2006)(1).

Intro. 2. Discovery of mutations in the TDP-43 gene in ALS/FTLD and the relation to prion protein. Most of the missense mutations (D169G to S393L) are located in the TDP-43 C-terminal regions (indicated by red bars). The region has been reported to have moderate sequence similarity with prion protein (highlighted by blue line) (21).

Intro. 3. Prion-like seeded aggregation of TDP-43.

(A) A schematic diagram of cellular localization TDP-43 in normal and diseased conditions. TDP-43 is localized in nuclei in a normal condition, whereas it is aggregated and localized in cytoplasms in degenerated neurons of ALS and FTLD patients. (B) Schematic diagrams of seeded aggregation of TDP-43 by prion-like conversion of normal

TDP-43 into an abnormal form.

Fig. 1. Construction of a series of partial deletion mutants of TDP-43 C-terminal fragment.

(A) Schematic diagrams of full-length TDP-43 and GFP-tagged TDP-CTF (162-414). Deletion sites (1~9) were designed on the 214~393 region of TDP-CTF. (B) Schematic diagrams of deletion mutants of TDP-CTF (Del 1~9). Each mutant possesses one of 9 deletions. Del 1 and 2 have deletions in RNA-recognition motif 2, Del 4 and 5 have deletions in the glycine-rich domain and Del 7,8 have deletions in the Q/N-rich domain. Deletion sites of Del 3 and 6 were designed to lie within gaps of domains and Del 9 was closest to the C-terminal.

Fig. 2. Immunoblot analysis of Sar-insoluble fraction of cells expressing TDP-CTF deletion mutants.

After 48 h incubation, SH-SY5Y cells transfected with TDP-CTF deletion mutants and WT (without deletion) were lysed in A68 buffer containing 1% Sar (Sar) and sequentially fractionated into Sar-soluble (sup) and Sar-insoluble (ppt) by centrifugation. These fractions were subjected to SDS-PAGE and proteins in gels were transferred to PVDF

membrane. Bands were detected with anti-GFP and anti-pS409/410 antibodies, and relative intensity (vs WT) is shown in the plot. Data are means ± SEM. (n = 3). *P < 0.05 by Student's t-test against the value of WT. (*p < 0.05 vs WT).

Fig. 3. Fluorescence microscopic analysis of aggregate formation of TDP-CTF deletion mutants expressed in cells.

(A) Fluorescence microscopic images of SH-SY5Y cells transfected with deletion mutants of TDP-CTF and WT. The fluorescence of GFP, which is fused to TDP-CTF, was detected. Aggregated TDP-CTF is distinguishable from diffusely expressed TDP-CTF, appearing as round or dot-like structures with much more intense GFP fluorescence. (B) Luminance extraction was conducted on acquired fluorescence microscopic images to quantify aggregate formation. To exclude fluorescence of non-aggregated protein, the lower limit of detectable GFP luminance level was adjusted so that only fluorescence of aggregated TDP-CTF was detected. Measured luminance was calculated as a relative value with respect to TDP-CTF WT. Data are means ± SEM. (n = 3). *P < 0.05 by Student`s t-test against the value of WT (*p < 0.05 vs WT).

Fig. 4. The effect of 40-amino-acid deletions on aggregate formation of TDP-CTF.

Deletion mutants of GFP-tagged TDP-CTF (162-414) were constructed with 40-amino-acid deletions at 234-273, 274-313, 314-353 and 354-393), and expressed in SH-SY5Y cells. TDP-43 deletion mutants collected in Sar-soluble (sup) and Sar-insoluble (ppt) fractions were detected with anti-GFP and anti-pS409/410 antibodies for GFP-tagged TDP-CTF series. Data are means ± SEM. (n = 3). *P < 0.05 by Student's t-test against the value of WT.

Fig. 5. Fluorescence microscopic analysis of aggregate formation of TDP-CTF 40-amino-acid deletion mutants expressed in cells.

Cells expressing GFP-tagged TDP-CTF deletion mutants (with 40-amino-acid deletions at 234-273, 274-313, 314-353 and 354-393) were observed by fluorescence microscopy and aggregate formation was quantified by luminance extraction of GFP fluorescence of aggregated TDP-CTF (D). Data are means ± SEM. (n = 3). *P < 0.05 by Student's t-test against the value of WT.

Fig. 6. The effect of 40-amino-acid deletions on aggregate formation of TDP-43

(ΔNLS &187-192).

Deletion mutants of TDP-43 (ΔNLS &187-192) were constructed with 40-amino-acid deletions at 234-273, 274-313, 314-353 and 354-393), and expressed in SH-SY5Y cells. TDP-43 deletion mutants collected in Sar-soluble (sup) and Sar-insoluble (ppt) fractions were detected with anti-TDP-43 and anti-pS409/410 antibodies for TDP-43 (ΔNLS &187-192) series.

Fig. 7. Synthetic peptides corresponding to sequences 234-273, 274-313, 314-353, 353-392.

Schematic diagrams of deletion sites on TDP-43 and sequences of 40-amino-acid synthetic peptides.

Fig. 8. *In vitro* aggregation of synthetic TDP-43 peptides (40 amino acid residues).

TDP-43 peptide solutions of 0.05 mM, 0.1 mM, 0.2 mM were prepared and incubated in 37℃ on a shaker. At the indicated time point, aliquots of peptide solution were added to 5μM thioflavin S (Th S) solution and Th S fluorescence was measured. Data are mean±SEM (n = 3).

Fig. 9. Electron microscopic analysis of aggregated TDP-43 peptides.

Peptide solutions after 8-day incubation at 37℃ on a shaker were loaded on a grid and negatively stained with phosphotungstate. Samples were observed under a transmission electron microscope. Magnification of acquired micrographs is 40,000x and scale bar = 100.0 nm.

Fig. 10. Synthetic peptide fibrils function as seeds in SH-SY5Y cells expressing full-length TDP-43.

TDP-43 peptide monomers (5 μg) without incubation (A) and fibrils prepared as described above (B) were introduced into cells immediately after transfection of full-length TDP-43. After incubation for 2 days, Sar-soluble (sup) and Sar-insoluble (ppt) fractions of cell lysate were prepared, and immunoblot analysis using anti-TDP-43 and anti-pS409/410 antibodies was conducted. Black arrowhead indicates abnormally phosphorylated TDP-43 of 45 kDa.

Fig. 11. The effect of phosphorylation of TDP-43 on seed-dependent aggregation.

Cells transfected with WT-TDP-43 and TDP-43 (Ser403/404/409/410 Ala) were treated with peptide fibrils of 274-313 and 314-353, and then immunoblotted using anti-TDP-43 and anti-TDP-43 (405-414).

Fig. 12. Immunocytochemical analysis of intracellular aggregation of TDP-43 induced by peptide fibrils.

Cells cultured on coverslips were transfected with expression plasmids of WT-TDP-43 and treated with TDP-43 peptide fibrils (234-273, 274-313 and 314-353). After 2 days of incubation, cells were fixed and stained with antibodies and nuclear staining dye (green: anti-TDP-43, red: anti-pS409/410, blue: TO-PRO-3). White arrow indicates abnormally phosphorylated cytoplasmic TDP-43 aggregates. Scale bar = 20 μm.

Fig. 13. Immunocytochemical analysis of intracellular aggregation of TDP-43(⊿NLS) induced by peptide fibrils.

Cells cultured on coverslips were transfected with expression plasmids of TDP-43(⊿NLS) and treated with TDP-43 peptide fibrils (234-273, 274-313 and 314-353). After 2 days of incubation, cells were fixed and stained with antibodies and nuclear staining dye (green: anti-TDP-43, red: anti-pS409/410, blue: TO-PRO-3). White arrow indicates abnormally phosphorylated cytoplasmic TDP-43 aggregates. Scale bar = 20 μm.

Fig. 14. Image analysis of cellar localization of abnormally phosphorylated TDP-43

aggregates.

Cytoplasmic localization of abnormally phosphorylated TDP-43 aggregates in WT-TDP-43 + fibril (274-313) cells was confirmed by image analysis. The locations of aggregates on single and merged images are surrounded by white lines (upper left panel). A magnified TO-PRO-3 image of the vicinity of the aggregates is shown in the upper right panel (with and without the white lines to indicate the location of aggregates). The lower panel and graph show the intensity distribution profiles of TDP-43 (green line), phosphorylated TDP-43 (red line) and TO-PRO-3 (blue line) along the indicated line.

Fig. 15. Different peptide fibrils generated different band patterns of TDP-43 C-terminal fragments and protease-resistant fragments.

Peptide fibrils of 274-313 and 314-353 were introduced into cells expressing WT-TDP-43 and ΔNLS-TDP-43 and aggregated TDP-43 contained in the Sar-insoluble fraction was detected by immunoblot analysis using anti- pS409/410 antibodies. (A) 22~28 kDa band patterns were compared between 274-313 and 314-353 peptide fibril-induced cells. Schematic diagrams of band patterns are indicated below the blot. (B) Sar-insoluble fractions were treated with 5 μg/mL trypsin for 30 min and then the reaction was stopped by heating at 100℃ for 5 min. Immunoblot analysis using anti-pS409/410 detected

remaining trypsin- resistant bands and their pattern is indicated as a schematic diagram below the blot.

Fig. 16. Comparison of TDP-43 in brains of patients with that in cells treated with peptide-fibril seeds.

Sar-insoluble fractions prepared from brains of patients (one case of FTD and one case of ALS) and from cells treated with peptide fibrils of 274-313 and 314-353 were digested with trypsin (10 μg/mL at 37℃ for 30 min). Untreated and trypsin-treated samples were immunoblotted with pS409/410.

Fig. 17. Cell death assay of cells containing intracellular aggregates following peptide-fibril introduction.

The extents of cell death in transfected and fibril-introduced cells were quantified by LDH assay. Cell death assay was conducted 2 days after treatment with peptide fibrils. Data are means ± SEM. (n = 3). *P < 0.05 by Student's t-test against the value of WT (*p < 0.05 vs WT).

Fig. 18. Seeding ability of peptide fibrils for TDP-43 deletion mutants.

(A) A series of deletion mutants of WT-TDP-43 lacking a 40 amino acid sequence of the C-terminal region were constructed and expressed in SH-SY5Y cells. After 48 h incubation, cells were fractionated into Sar-soluble (sup) and Sar-insoluble (ppt). Immunoblotting of sup was conducted using anti-TDP-43 and immunoblotting of ppt was conducted using anti-pS409/410 antibodies. (B) TDP-43 peptide fibrils of 274-313 (B) and 314-353 (C) were introduced into cells expressing these WT-TDP-43 deletion mutants. The sup and ppt fractions were prepared and immunoblotted. Black arrowhead indicates endogenous full-length TDP-43 and white arrowhead indicates deletion mutant of TDP-43.

Fig. 19. Sequence similarity between TDP-43 C-terminal regions and PrP.

Based on a report of moderate similarity between C-terminal regions of TDP-43 and PrP (21), regions corresponding to TDP-43 (234-273, 274-313, 314-353) are indicated on the alignment of human TDP-43 C-terminal region and human PrP.

Fig. 20. Schematic diagram of the locations of aggregation-associated sequences of

TDP-43.

Aggregation-associated sequences of TDP-43 identified in this study and previous reports are displayed on the diagram of TDP-43. Sequences are indicated by bars in a schematic diagram of the TDP-43 C-terminal region.

Reference

1. Arai, T., Hasegawa, M., Akiyama, H., Ikeda, K., Nonaka, T., Mori, H., Mann, D., Tsuchiya, K., Yoshida, M., Hashizume, Y., Oda, T. (2006) TDP-43 is a component of ubiquitin-positive tau-negative inclusions in frontotemporal lobar degeneration and amyotrophic lateral sclerosis. Biochem. Biophys. Res. Commun. 351, 602-11
2. Neumann, M., Sampathu, D.M., Kwong, L.K., Truax, A.C., Micsenyi, M.C., Chou, T.T., Bruce, J., Schuck, T., Grossman, M., Clark, C.M., McCluskey, L.F., Miller, B.L., Masliah, E., Mackenzie, I.R., Feldman, H., Feiden, W., Kretzschmar, H.A., Trojanowski, J.Q., Lee, V.M. (2006) Ubiquitinated TDP-43 in frontotemporal lobar degeneration and amyotrophic lateral sclerosis. Science 314, 130-3
3. Ou, S.H., Wu, F., Harrich, D., Garcia-Martinez, L.F., Gaynor, R.B. (1995) Cloning and characterization of a novel cellular protein, TDP-43, that binds to human immunodeficiency virus type 1 TAR DNA sequence motifs. J Virol. 69, 3584-96
4. Buratti, E., Dork, T., Zuccato, E., Pagani, F., Romano, M., Baralle, F.E. (2001) Nuclear factor TDP-43 and SR proteins promote in vitro and in vivo CFTR exon 9 skipping. EMBO J. 20, 1774-84

5. Daoud, H., Valdmanis, P.N., Kabashi, E., Dion, P., Dupre, N., Camu, W., Meininger, V., Rouleau, G.A. (2009) Contribution of TARDBP mutations to sporadic amyotrophic lateral sclerosis. J. Med. Genet. 46, 112-4

6. Gitcho, M.A., Baloh, R.H., Chakraverty, S., Mayo, K., Norton, J.B., Levitch, D., Hatanpaa, K.J., White, C.L. 3rd, Bigio, E.H., Caselli, R., Baker, M., Al-Lozi, M.T., Morris, J.C., Pestronk, A., Rademakers, R., Goate, A.M., Cairns, N.J. (2008) TDP-43 A315T mutation in familial motor neu ron disease. Ann. Neurol. 63, 535-8

7. Kabashi, E., Valdmanis, P.N., Dion, P., Spiegelman, D., McConkey, B.J., Vande Velde, C., Bouchard, J.P., Lacomblez, L., Pochigaeva, K., Salachas, F., Pradat, P.F., Camu, W., Meininger, V., Dupre, N., Rouleau, G.A. (2008) TARDBP mutations in individuals with sporadic and familial amyotrophic lateral sclerosis. Nat. Genet. 40, 572-4.

8. Kuhnlein, P., Sperfeld, A.D., Vanmassenhove, B., Van Deerlin, V., Lee, V.M., Trojanowski, J.Q., Kretzschmar, H.A., Ludolph, A.C., Neumann, M. (2008) Two German kindreds with familial amyotrophic lateral sclerosis due to TARDBP mutations. Arch. Neurol. 65, 1185-9.

9. Rutherford, N.J., Zhang, Y.J., Baker, M., Gass, J.M., Finch, N.A., Xu, Y.F.,

Stewart, H., Kelley, B.J., Kuntz, K., Crook, R.J., Sreedharan, J., Vance, C., Sorenson, E., Lippa, C., Bigio, E.H., Geschwind, D.H., Knopman, D.S., Mitsumoto, H., Petersen, R.C., Cashman, N.R., Hutton, M., Shaw, C.E., Boylan, K.B., Boeve, B., Graff-Radford, N.R., Wszolek, Z.K., Caselli, R.J., Dickson, D.W., Mackenzie, I.R., Petrucelli, L., Rademakers, R. (2008) Novel mutations in TARDBP (TDP-43) in patients with familial amyotrophic lateral sclerosis. PLoS Genet. 4, e1000193.

10. Sreedharan, J., Blair, I.P., Tripathi, V.B., Hu, X., Vance, C., Rogelj, B., Ackerley, S., Durnall, J.C., Williams, K.L., Buratti, E., Baralle, F., de Belleroche, J., Mitchell, J.D., Leigh, P.N., Al-Chalabi, A., Miller, C.C., Nicholson, G., Shaw, C.E. (2008) TDP-43 mutations in familial and sporadic amyotrophic lateral sclerosis. Science 319, 1668-72.

11. Van Deerlin, V.M., Leverenz, J.B., Bekris, L.M., Bird, T.D., Yuan, W., Elman, L.B., Clay, D., Wood, E.M., Chen-Plotkin, A.S., Martinez-Lage, M., Steinbart, E., McCluskey, L., Grossman, M., Neumann, M., Wu, I.L., Yang, W.S., Kalb, R., Galasko, D.R., Montine, T.J., Trojanowski, J.Q., Lee, V.M., Schellenberg, G.D., Yu, C.E. (2008) TARDBP mutations in amyotrophic lateral sclerosis with TDP-43 neuropathology: a genetic and histopathological analysis. Lancet Neurol. 7,

409-16.

12. Yokoseki, A., Shiga, A., Tan, C.F., Tagawa, A., Kaneko, H., Koyama, A., Eguchi, H., Tsujino, A., Ikeuchi, T., Kakita, A., Okamoto, K., Nishizawa, M., Takahashi, H., Onodera, O., TDP-43 mutation in familial amyotrophic lateral sclerosis. Ann Neurol. 2008; 63: 538-42.
13. Hasegawa, M., Arai, T., Nonaka, T., Kametani, F., Yoshida, M., Hashizume, Y., Beach, T.G., Buratti, E., Baralle, F., Morita, M., Nakano, I., Oda, T., Tsuchiya, K., Akiyama, H. (2008) Phosphorylated TDP-43 in frontotemporal lobar degeneration and amyotrophic lateral sclerosis. Ann. Neurol. 64, 60-70.
14. Mackenzie, I.R., Neumann, M., Baborie, A., Sampathu, D.M., Du Plessis, D., Jaros, E., Perry, R.H., Trojanowski, J.Q., Mann, D.M., Lee, V.M. (2011) A harmonized classification system for FTLD-TDP pathology. Acta Neuropathol. 122, 111-3.
15. Tsuji, H., Arai, T., Kametani, F., Nonaka, T., Yamashita, M., Suzukake, M., Hosokawa, M., Yoshida, M., Hatsuta, H., Takao, M., Saito, Y., Murayama, S., Akiyama, H., Hasegawa, M., Mann, D.M., Tamaoka, A. (2012) Molecular analysis and biochemical classification of TDP-43 proteinopathy. Brain 135, 3380-91.

16. Nonaka, T., Masuda-Suzukake, M., Arai, T., Hasegawa, Y., Akatsu, H., Obi, T., Yoshida, M., Hasegawa, M. (2013) Prion-like properties of pathological TDP-43 aggregates from diseased brains. Cell Rep. 4, 124-34.

17. Nonaka, T., Kametani, F., Arai, T., Akiyama, H., Hasegawa, M. (2009) Truncation and pathogenic mutations facilitate the formation of intracellular aggregates of TDP-43. Hum. Mol. Genet. 18, 3353-64.

18. Nonaka, T., Arai, T., Buratti, E., Baralle, F.E., Akiyama, H., Hasegawa, M. (2009) Phosphorylated and ubiquitinated TDP-43 pathological inclusions in ALS and FTLD-U are recapitulated in SH-SY5Y cells. FEBS Lett. 583, 394-400.

19. Inukai, Y., Nonaka, T., Arai, T., Yoshida, M., Hashizume, Y., Beach, T.G., Buratti, E., Baralle, F.E., Akiyama, H., Hisanaga, S., Hasegawa, M. (2008) Abnormal phosphorylation of Ser409/410 of TDP-43 in FTLD-U and ALS. FEBS Lett. 582, 2899-904.

20. Masuda-Suzukake, M., Nonaka, T., Hosokawa, M., Oikawa, T., Arai, T., Akiyama, H., Mann, D.M., Hasegawa, M. (2013) Prion-like spreading of pathological α-synuclein in brain. Brain 136, 1128-38.

21. Guo, W., Chen, Y., Zhou, X., Kar, A., Ray, P., Chen, X., Rao, E.J., Yang, M., Ye, H., Zhu, L., Liu, J., Xu, M., Yang, Y., Wang, C., Zhang, D., Bigio, E.H., Mesulam,

M., Shen, Y., Xu, Q., Fushimi, K., Wu, J.Y. (2011) An ALS-associated mutation affecting TDP-43 enhances protein aggregation, fibril formation and neurotoxicity. Nat. Struct. Mol. Biol. 18, 822-30.

22. Jiang, L.L., Che, M.X., Zhao, J., Zhou, C.J., Xie, M.Y., Li, H.Y., He, J.H., Hu, H.Y. (2013) Structural transformation of the amyloidogenic core region of TDP-43 protein initiates its aggregation and cytoplasmic inclusion. J. Biol. Chem. 288, 19614-24.
23. Wang, Y.T., Kuo, P.H., Chiang, C.H., Liang, J.R., Chen, Y.R., Wang, S., Shen, J.C., Yuan, H.S. (2013) The truncated C-terminal RNA recognition motif of TDP-43 protein plays a key role in forming proteinaceous aggregates. J. Biol. Chem. 288, 9049-57.
24. Saini, A., Chauhan, V.S. (2011) Delineation of the core aggregation sequences of TDP-43 C-terminal fragment. Chembiochem. 12, 2495-501.
25. Furukawa, Y., Kaneko, K., Watanabe, S., Yamanaka, K., Nukina, N. (2011) J. Biol. Chem. 286, 18664-72.
26. Chen, A.K., Lin, R.Y., Hsieh, E.Z., Tu, P.H., Chen, R.P., Liao, T.Y., Chen, W., Wang, C.H., Huang, J.J. (2010) Induction of amyloid fibrils by the C-terminal fragments of TDP-43 in amyotrophic lateral sclerosis. J. Am. Chem. Soc. 132,

1186-7.

27. Sun, C.S., Wang, C.Y., Chen, B.P., He, R.Y., Liu, G.C., Wang, C.H., Chen, W., Chern, Y., Huang, J.J. (2014) The influence of pathological mutations and proline substitutions in TDP-43 glycine-rich peptides on its amyloid properties and cellular toxicity. PLoS One. 9, e103644.
28. Berriman, J., Serpell, L.C., Oberg, K.A., Fink, A.L., Goedert, M., Crowther, R.A. (2003) Tau filaments from human brain and from in vitro assembly of recombinant protein show cross-beta structure. Proc. Natl. Acad. Sci. USA. 100, 9034-8.
29. Serpell, L.C., Berriman, J., Jakes, R., Goedert, M., Crowther, R.A. (2000) Fiber diffraction of synthetic alpha-synuclein filaments shows amyloid-like cross-beta conformation. Proc. Natl. Acad. Sci. USA. 97, 4897-902.
30. Nonaka, T., Watanabe, S.T., Iwatsubo, T., Hasegawa, M. (2010) Seeded aggregation and toxicity of {alpha}-synuclein and tau: cellular models of neurodegenerative diseases. J. Biol. Chem. 285, 34885-98.

Acknowledgements

I would like to thank Dr. Masato Hasegawa at Tokyo Metropolitan Institute of Medical Science for technical instruction, considerable discussion.

I would like to thank Dr. Shin-ichi Hisanaga at Tokyo Metropolitan University for insightful advice.

I wish to thank Dr. Takashi Nonaka and Dr. Genjiro Suzuki at Tokyo Metropolitan Institute of Medical Science for technical instruction, and helpful advice.

I thank my laboratory members for helpful discussion and encouragement.

A

TAR DNA-binding protein of 43kDa (TDP-43)

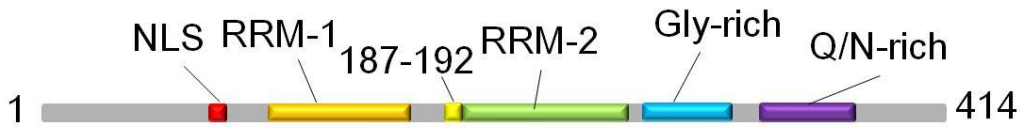

B

ALS (spinal code)

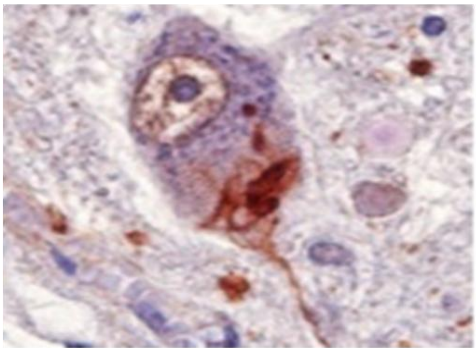

(Arai et al., 2006)

FTLD (hippocampus)

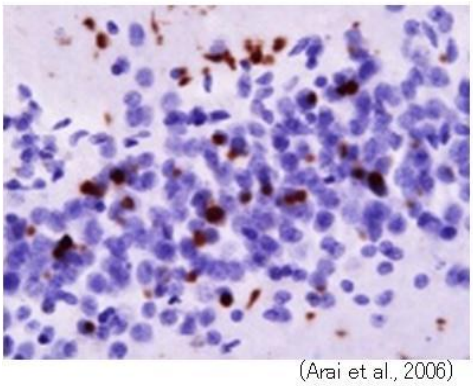

(Arai et al., 2006)

Intro. 1

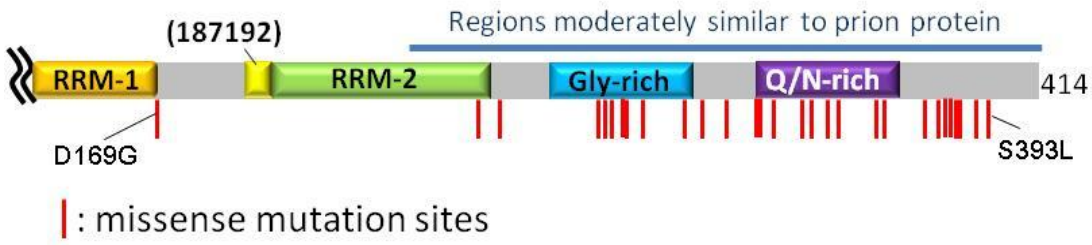
(187192)
Regions moderately similar to prion protein
RRM-1
RRM-2
Gly-rich
Q/N-rich
414
D169G
S393L
: missense mutation sites

Intro. 2

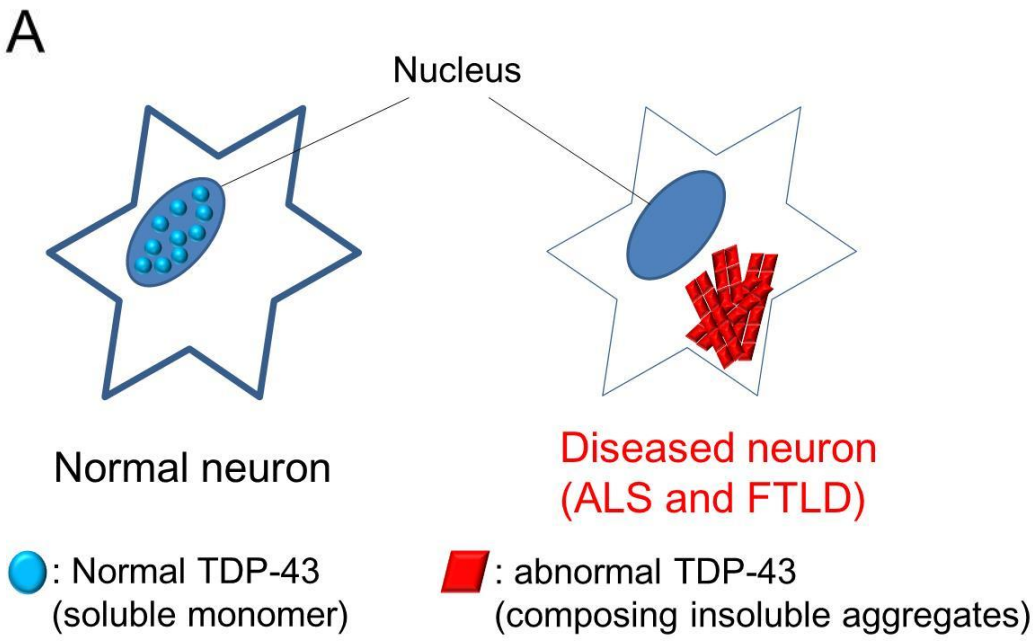
A
Nucleus
Normal neuron
Diseased neuron
(ALS and FTLD)
: Normal TDP-43
(soluble monomer)
: abnormal TDP-43
(composing insoluble aggregates)

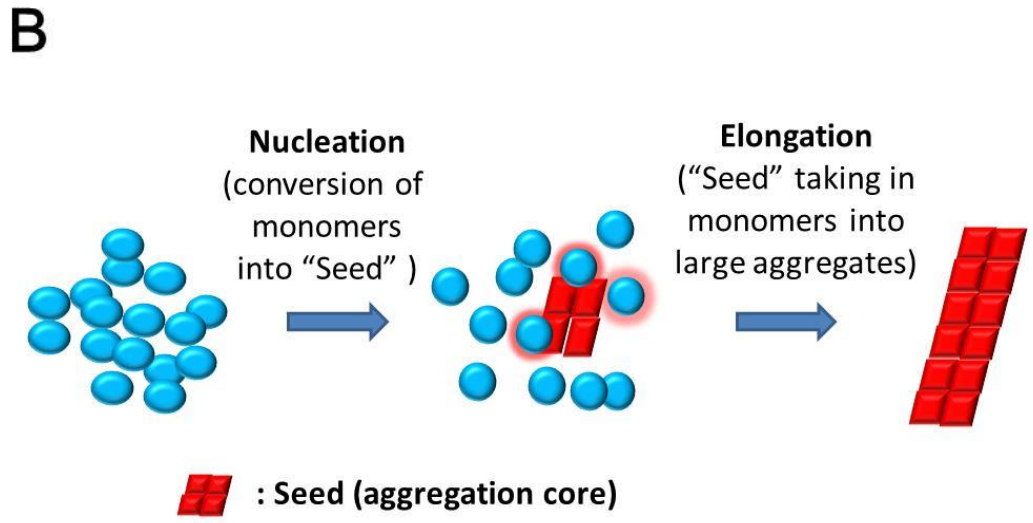
B
Nucleation
(conversion of
monomers
into "Seed")
Elongation
("Seed" taking in
monomers into
large aggregates)
: Seed (aggregation core)

Intro. 3

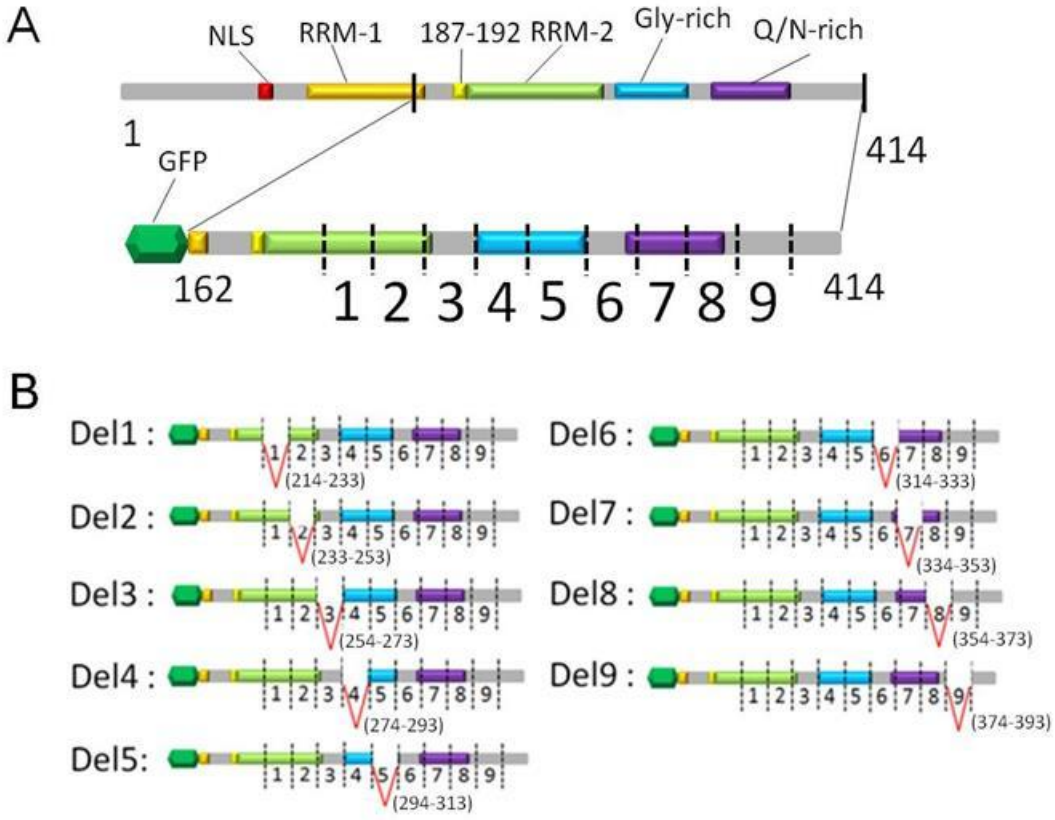
A
NLS
RRM-1
187-192
RRM-2
Gly-rich
Q/N-rich
1
414
GFP
162
1 2 3 4 5 6 7 8 9
414
B
Del1 :
(214-233)
Del2 :
(233-253)
Del3 :
(254-273)
Del4 :
(274-293)
Del5:
(294-313)
Del6 :
(314-333)
Del7 :
(334-353)
Del8 :
(354-373)
Del9 :
(374-393)

Fig. 1

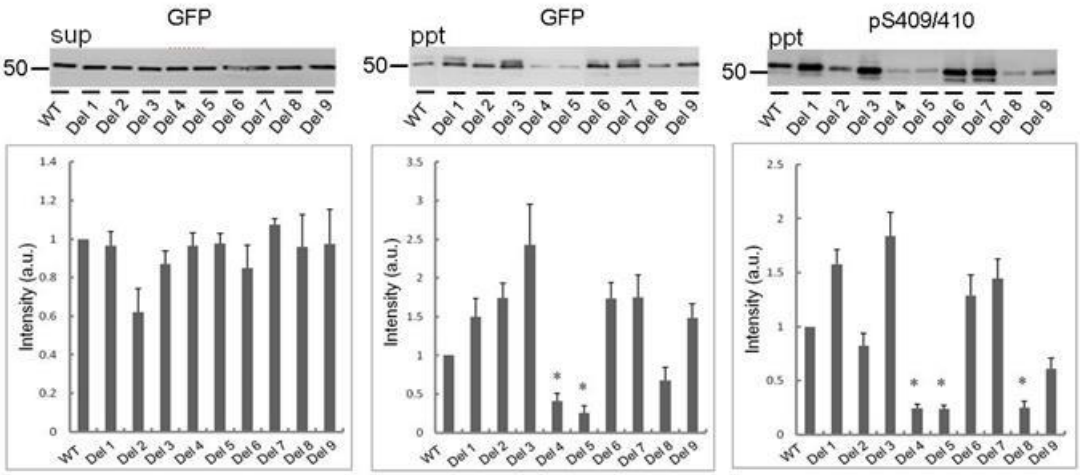
GFP
sup
50
WT
Del 1
Del 2
Del 3
Del 4
Del 5
Del 6
Del 7
Del 8
Del 9
Intensity (a.u.)
GFP
ppt
pS409/410
ppt

Fig. 2

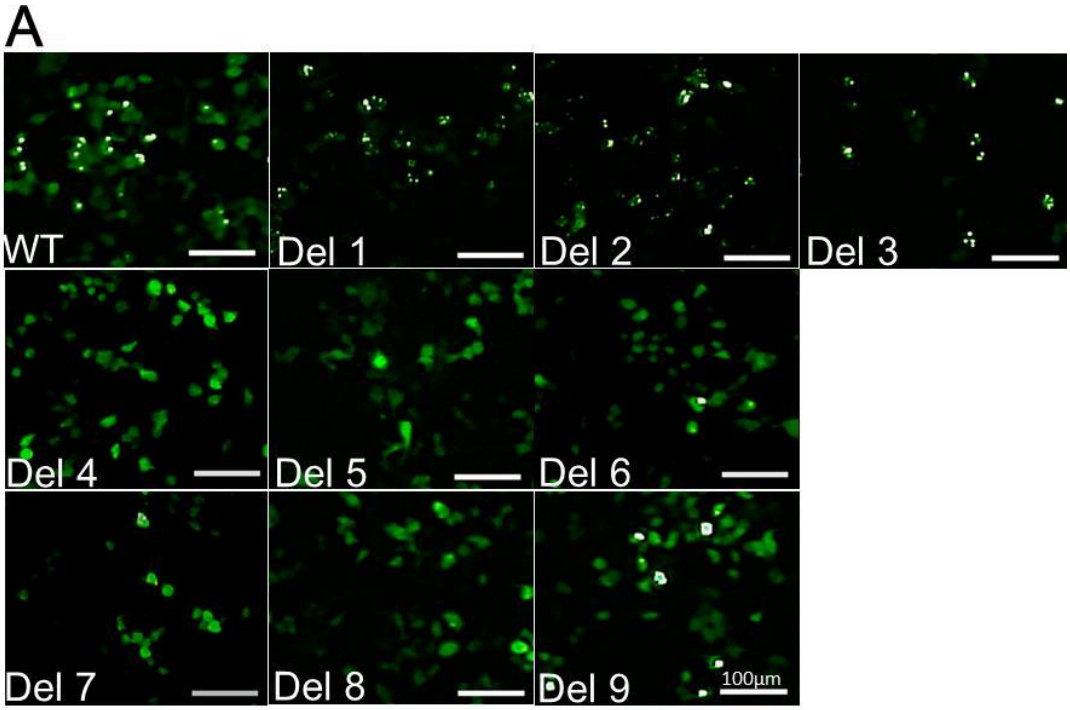
A
WT
Del 1
Del 2
Del 3
Del 4
Del 5
Del 6
Del 7
Del 8
Del 9
100μm

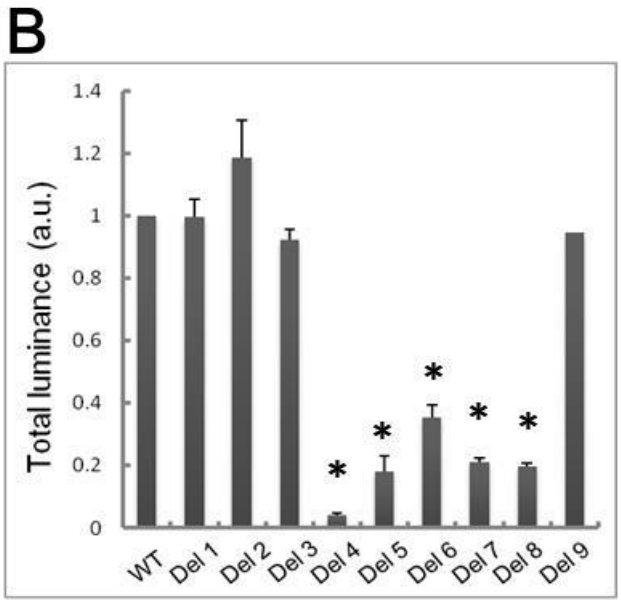
B
Total luminance (a.u.)
1.4
1.2
1
0.8
0.6
0.4
0.2
0
WT
Del 1
Del 2
Del 3
Del 4
Del 5
Del 6
Del 7
Del 8
Del 9
*

Fig. 3

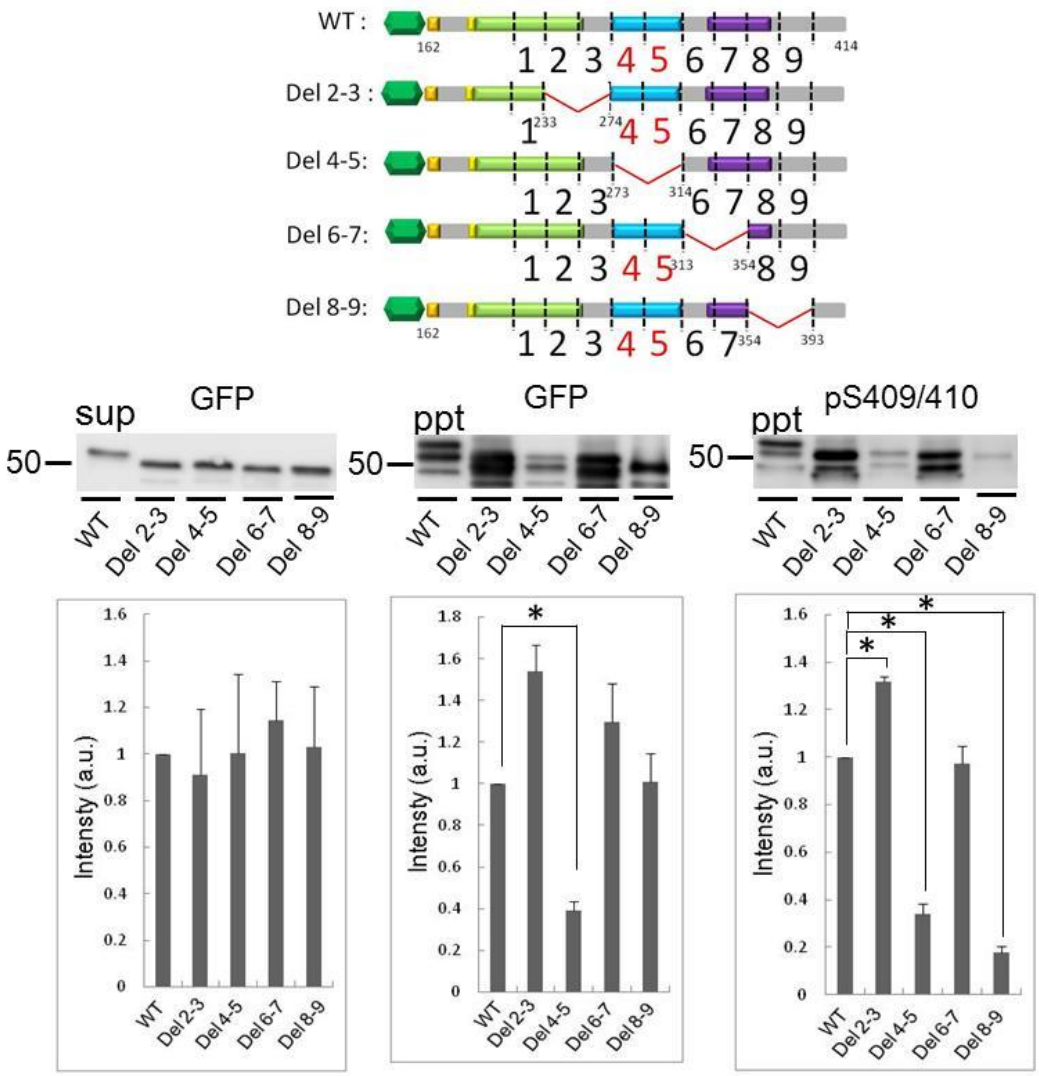
WT :
Del 2-3 :
Del 4-5:
Del 6-7:
Del 8-9:
sup
GFP
ppt
GFP
ppt
pS409/410
50
WT
Del 2-3
Del 4-5
Del 6-7
Del 8-9
Intensty (a.u.)

Fig. 4

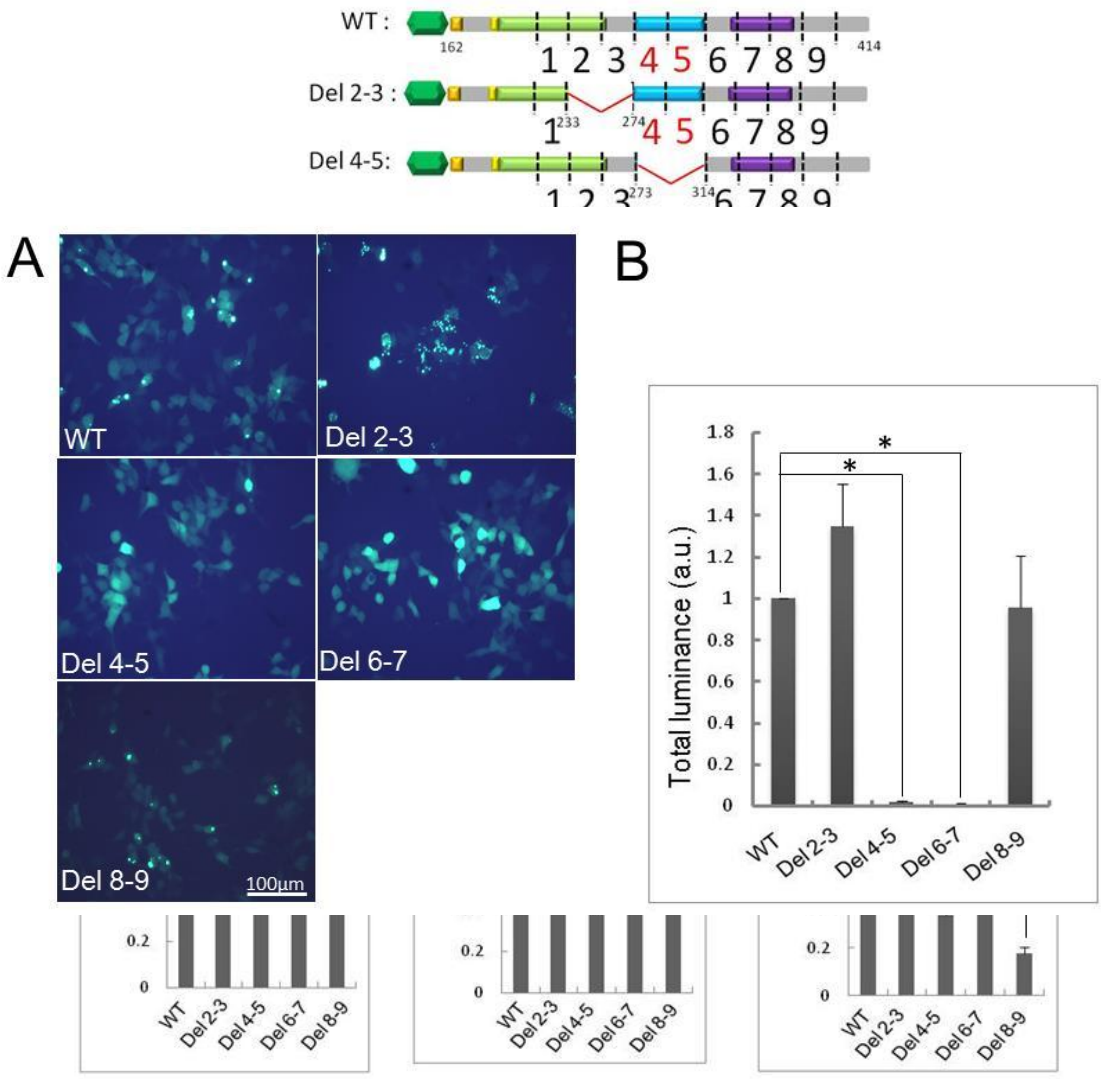
WT :
162
1 2 3 4 5 6 7 8 9
414
Del 2-3 :
1
233
274
4 5 6 7 8 9
Del 4-5:
273
314
A
B
WT
Del 2-3
Del 4-5
Del 6-7
Del 8-9
100μm
Total luminance (a.u.)
1.8
1.6
1.4
1.2
1
0.8
0.6
0.4
0.2
0
*
*
WT
Del2-3
Del4-5
Del6-7
Del8-9

Fig. 5

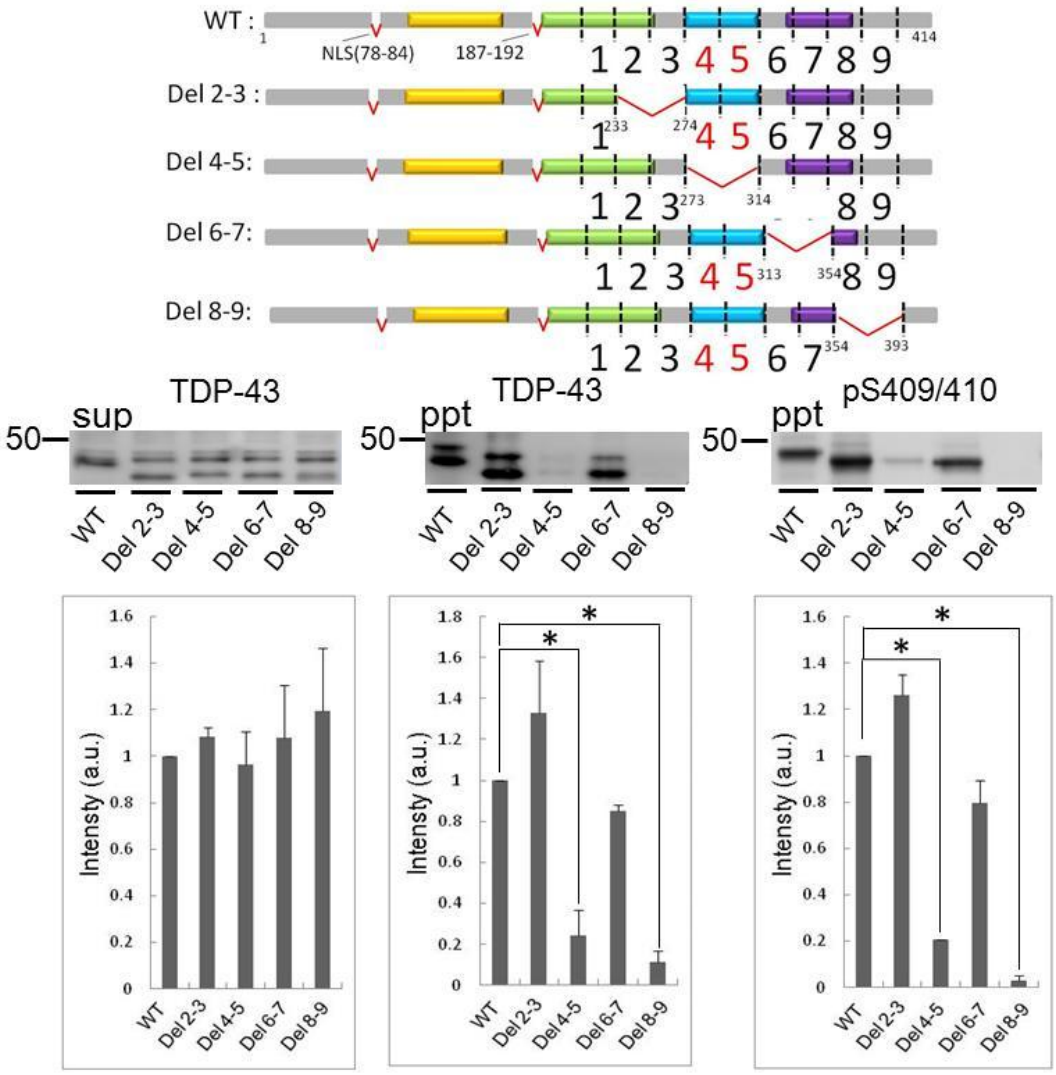
WT :
NLS(78-84)
187-192
1 2 3 4 5 6 7 8 9
Del 2-3 :
Del 4-5:
Del 6-7:
Del 8-9:
TDP-43
sup
TDP-43
ppt
pS409/410
ppt
50
WT
Del 2-3
Del 4-5
Del 6-7
Del 8-9
Intensty (a.u.)

Fig. 6

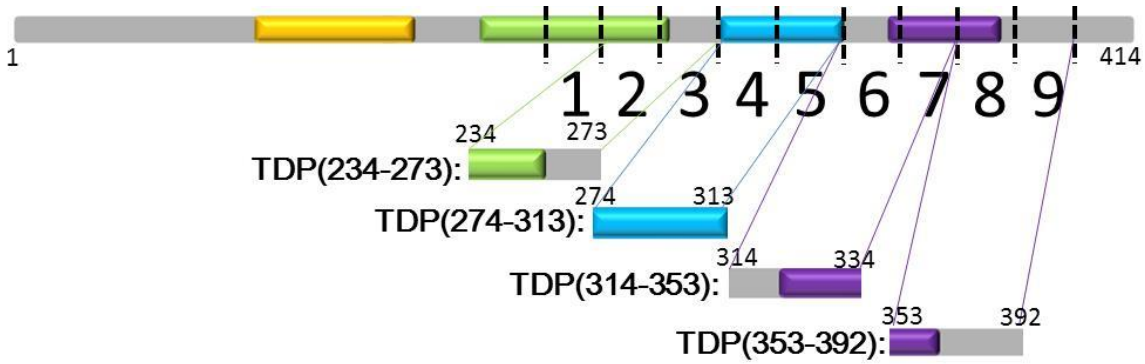

TDP(234-273): FADDQIAQSLCGEDLIIKGISVHISNAEPKHNSNRQLERS
TDP(274-313): GRFGGNPGGFGNQGGFGNSRGGGAGLGNNQGSNMGGGMNF
TDP(314-353): GAFSINPAMMAAAQAALQSSWGMMGMLASQQNQSGPSGNN
TDP(353-392): NQNQGNMQREPNQAFGSGNNSYSGSNSGAAIGWGSASNAG
Control: NHYVKMILKKALSRYPNRRNLPCVDLRYKRKSIILQRKYS

Fig. 7

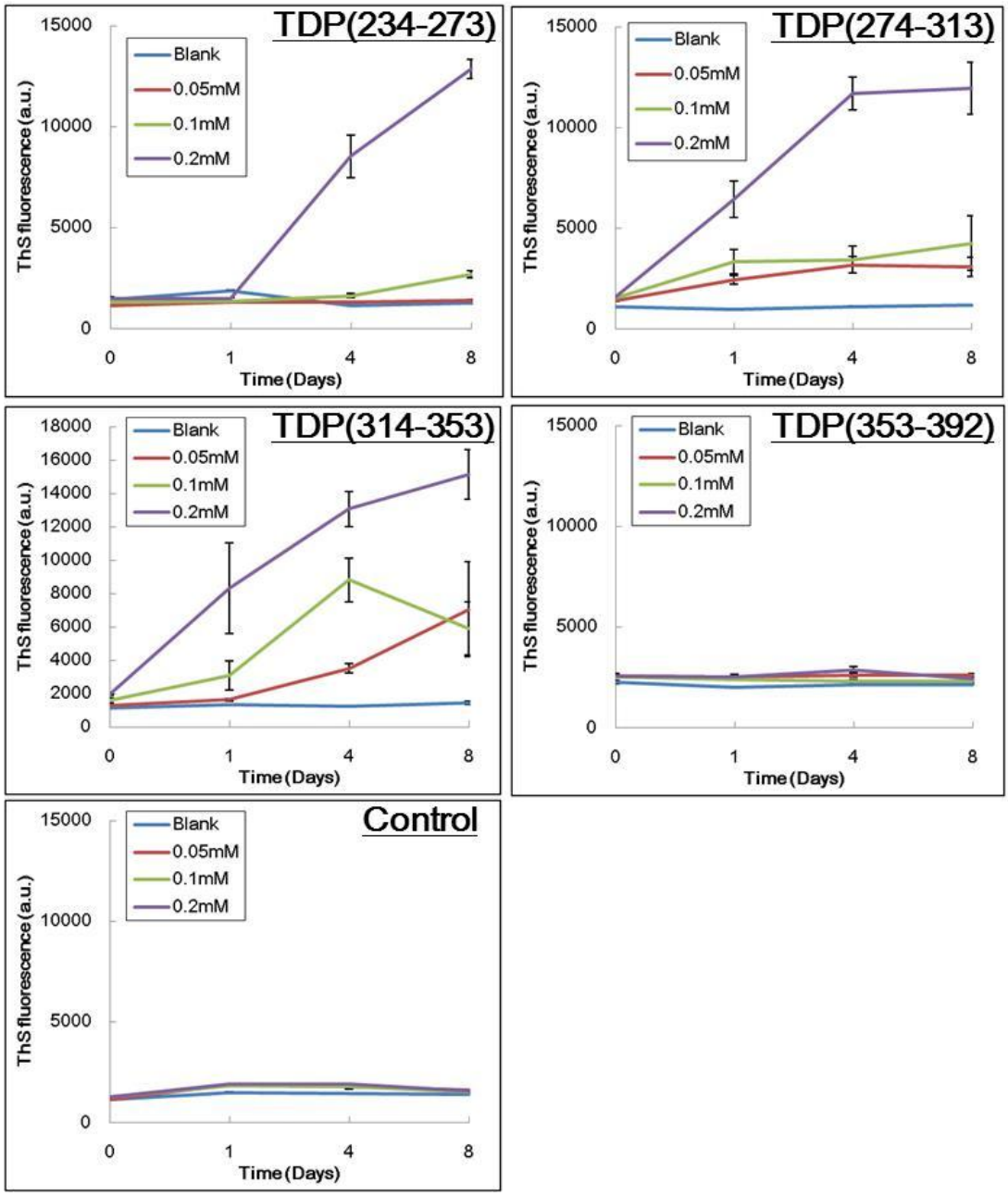
TDP(234-273)
TDP(274-313)
TDP(314-353)
TDP(353-392)
Control
Blank
0.05mM
0.1mM
0.2mM
ThS fluorescence (a.u.)
Time (Days)
0
1
4
8
0
5000
10000
15000
2000
4000
6000
8000
12000
14000
16000
18000

Fig. 8

TDP-43(234-273)

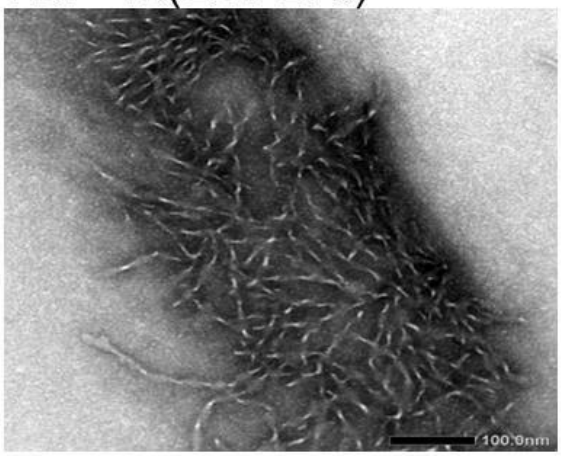

TDP-43(274-313)

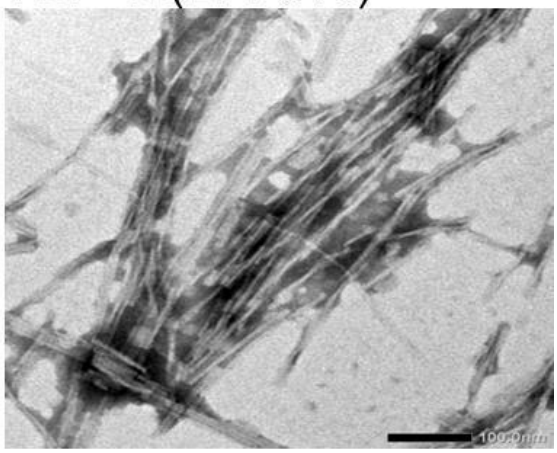

TDP-43(314-353)

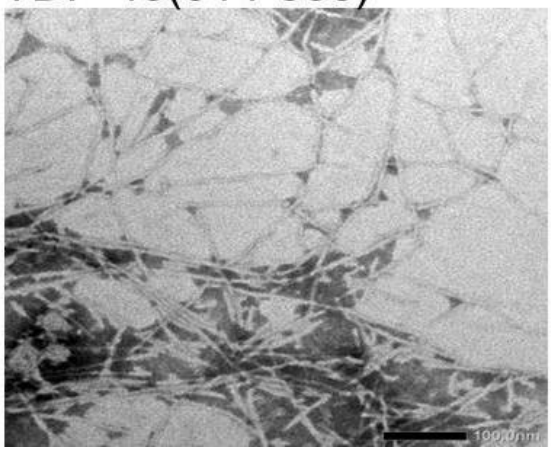

Fig. 9

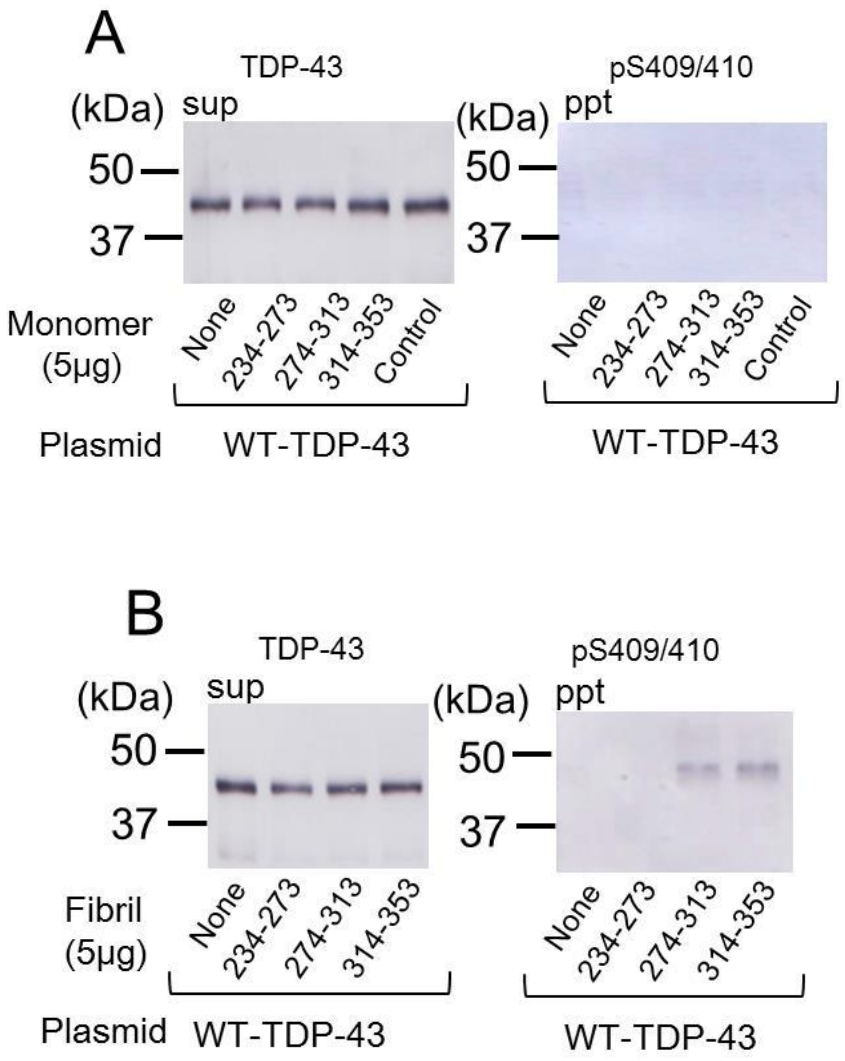
A
TDP-43
pS409/410
(kDa)
sup
(kDa)
ppt
50
37
50
37
Monomer
(5μg)
None
234-273
274-313
314-353
Control
None
234-273
274-313
314-353
Control
Plasmid
WT-TDP-43
WT-TDP-43
B
TDP-43
pS409/410
(kDa)
sup
(kDa)
ppt
50
37
50
37
Fibril
(5μg)
None
234-273
274-313
314-353
None
234-273
274-313
314-353
Plasmid
WT-TDP-43
WT-TDP-43

Fig. 10

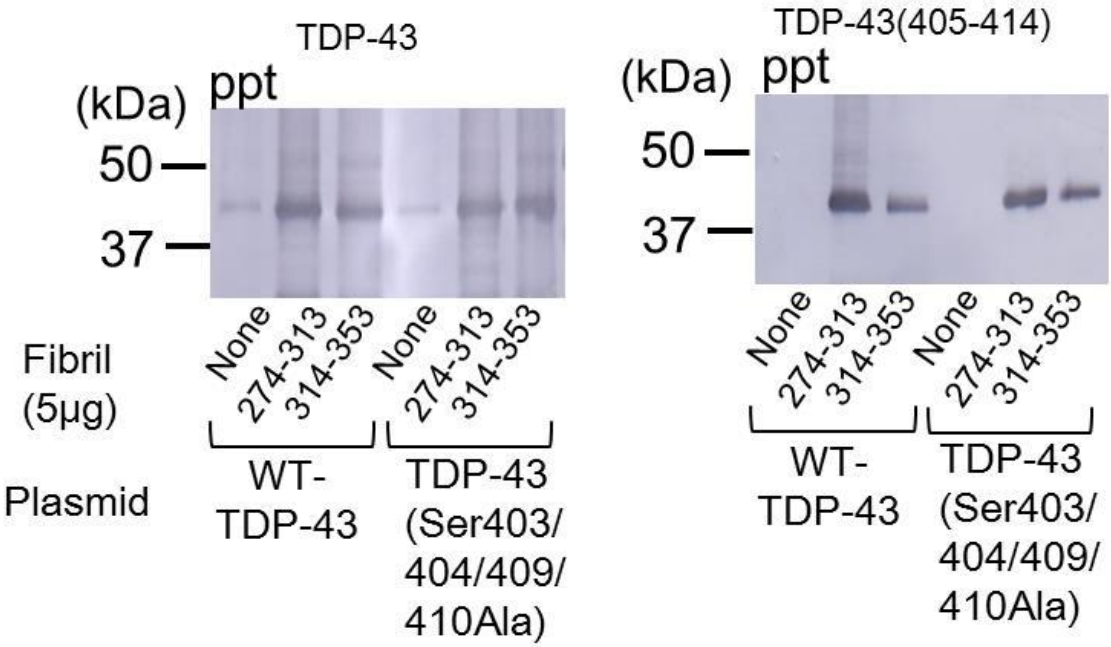
TDP-43
(kDa)
ppt
50
37
None
274-313
314-353
None
274-313
314-353
Fibril
(5μg)
Plasmid
WT-
TDP-43
TDP-43
(Ser403/
404/409/
410Ala)
TDP-43(405-414)
(kDa)
ppt
50
37
None
274-313
314-353
None
274-313
314-353
WT-
TDP-43
TDP-43
(Ser403/
404/409/
410Ala)

Fig. 11

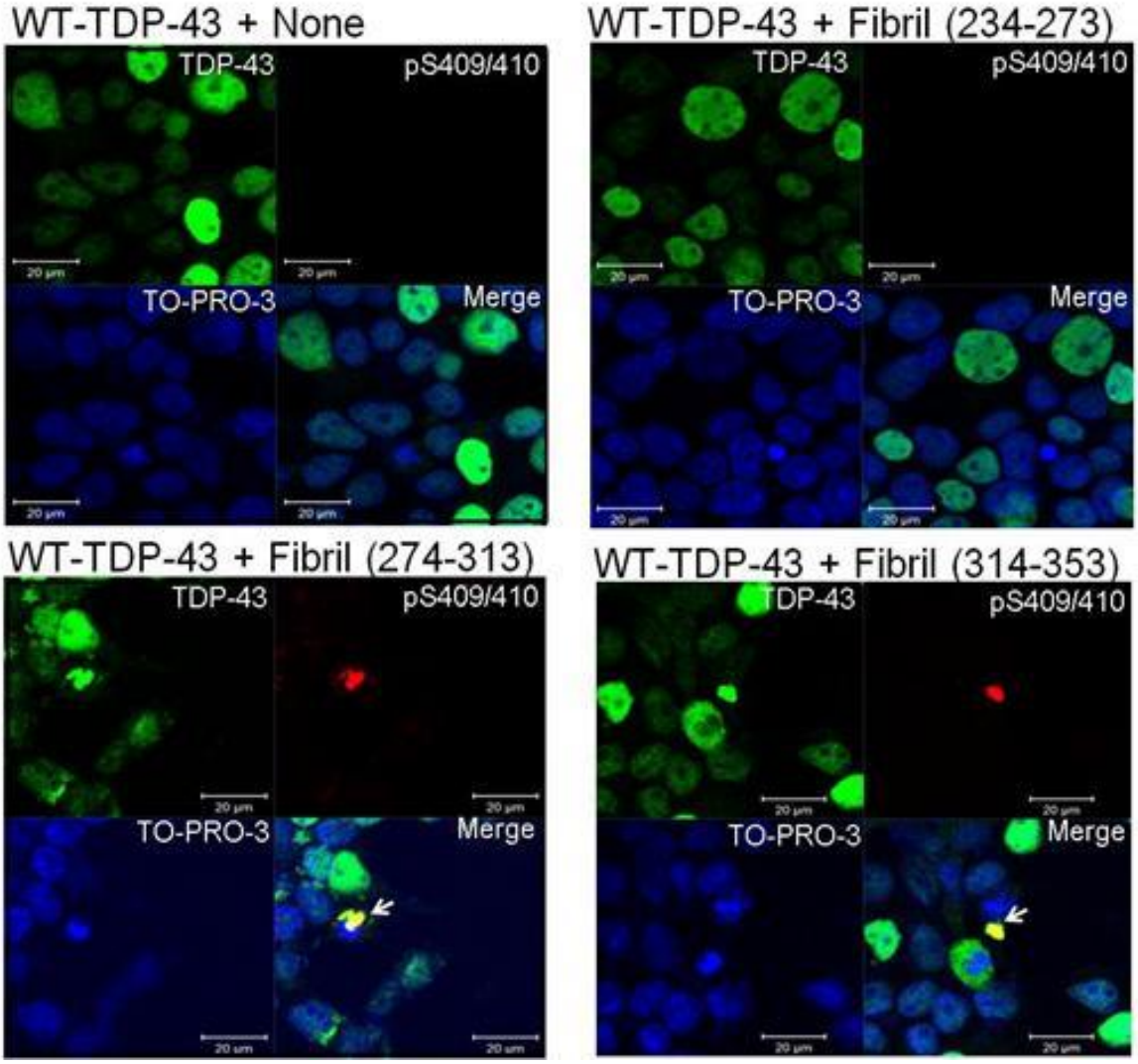
WT-TDP-43 + None
TDP-43
pS409/410
TO-PRO-3
Merge
WT-TDP-43 + Fibril (234-273)
TDP-43
pS409/410
TO-PRO-3
Merge
WT-TDP-43 + Fibril (274-313)
TDP-43
pS409/410
TO-PRO-3
Merge
WT-TDP-43 + Fibril (314-353)
TDP-43
pS409/410
TO-PRO-3
Merge

Fig. 12

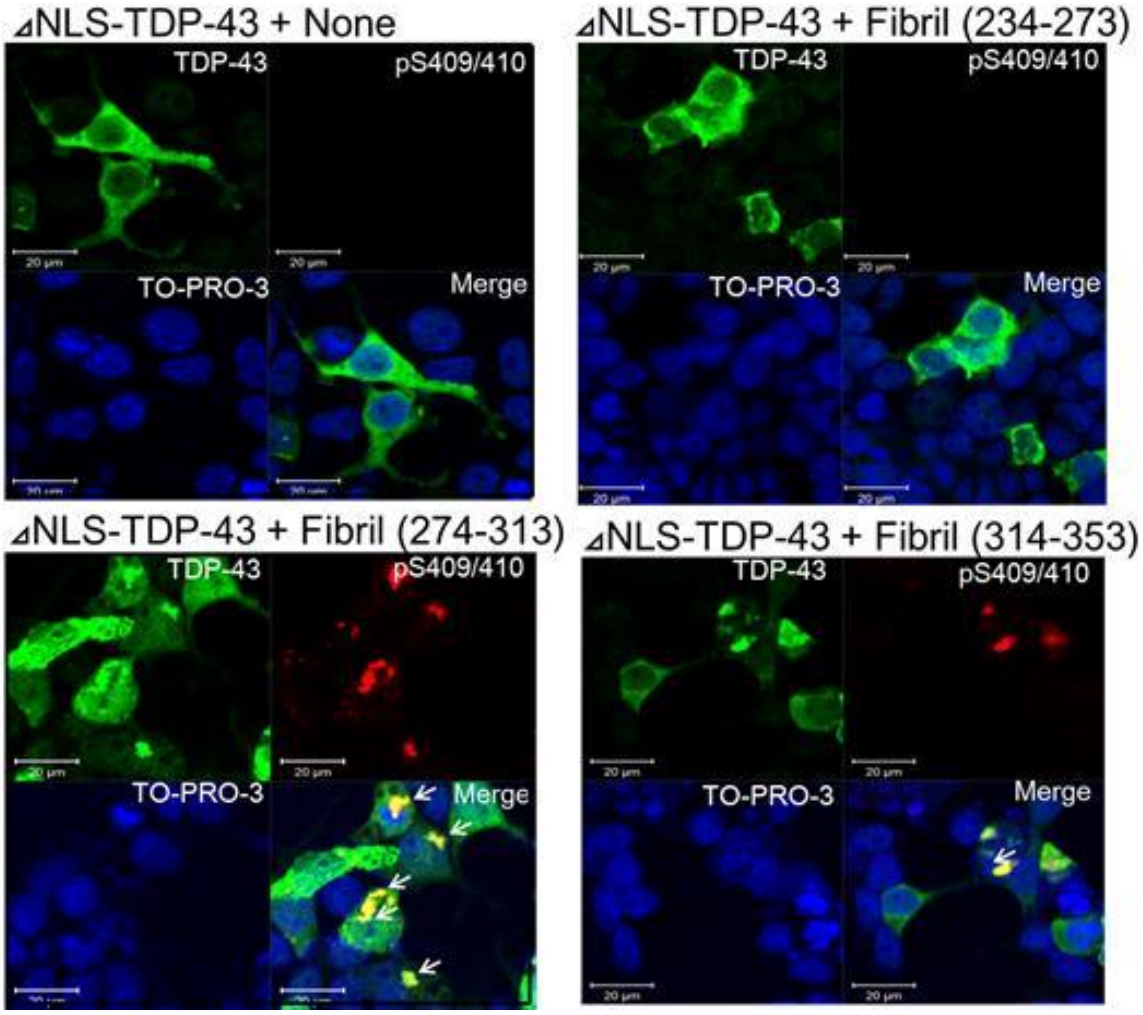
ΔNLS-TDP-43 + None
TDP-43
pS409/410
TO-PRO-3
Merge
ΔNLS-TDP-43 + Fibril (234-273)
TDP-43
pS409/410
TO-PRO-3
Merge
ΔNLS-TDP-43 + Fibril (274-313)
TDP-43
pS409/410
TO-PRO-3
Merge
ΔNLS-TDP-43 + Fibril (314-353)
TDP-43
pS409/410
TO-PRO-3
Merge

Fig. 13

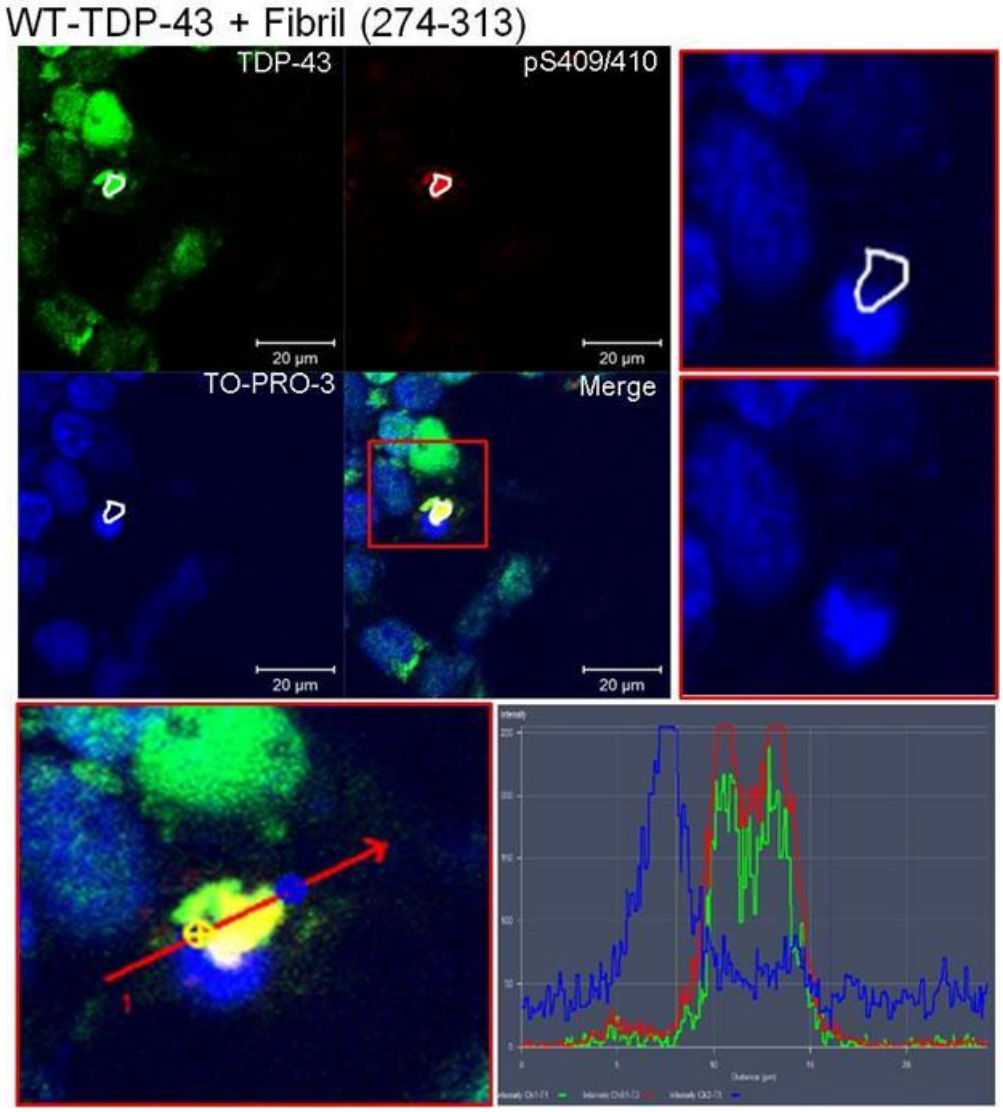
WT-TDP-43 + Fibril (274-313)
TDP-43
pS409/410
TO-PRO-3
Merge
20 µm
20 µm
20 µm
20 µm

Fig. 14

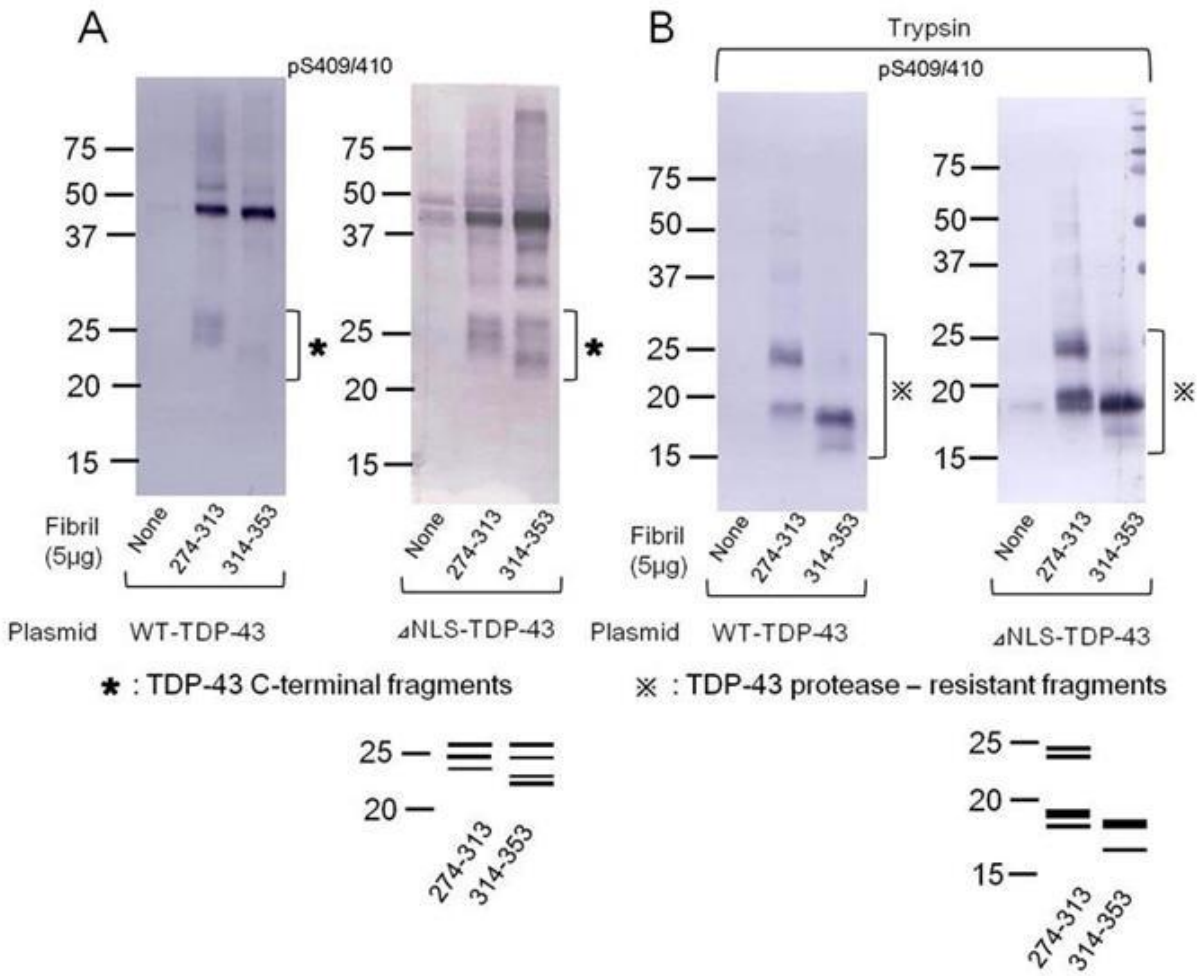
A
pS409/410
75
50
37
25
20
15
*
Fibril (5μg)
None
274-313
314-353
Plasmid
WT-TDP-43
⊿NLS-TDP-43
B
Trypsin
pS409/410
※
* : TDP-43 C-terminal fragments
※ : TDP-43 protease – resistant fragments

Fig. 15

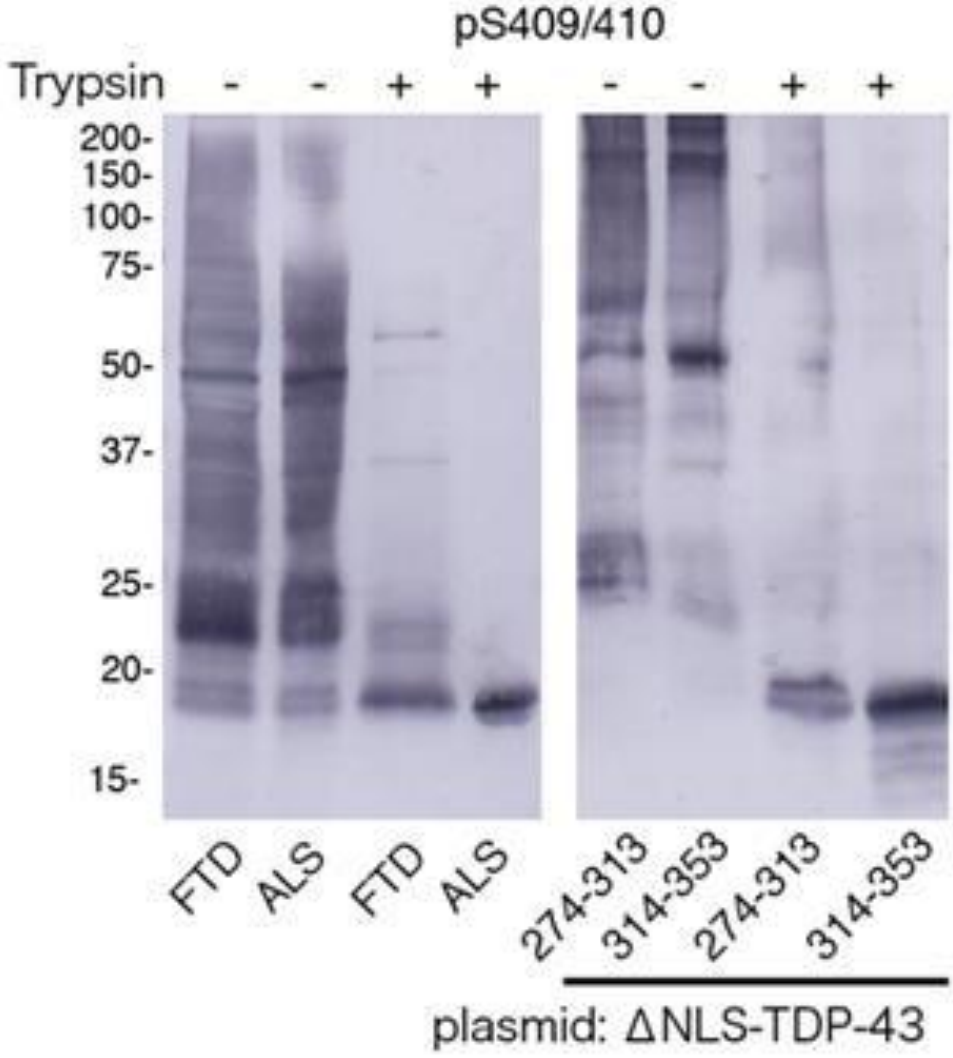
pS409/410
Trypsin - - + + - - + +
200-
150-
100-
75-
50-
37-
25-
20-
15-
FTD
ALS
FTD
ALS
274-313
314-353
274-313
314-353
plasmid: ΔNLS-TDP-43

Fig. 16

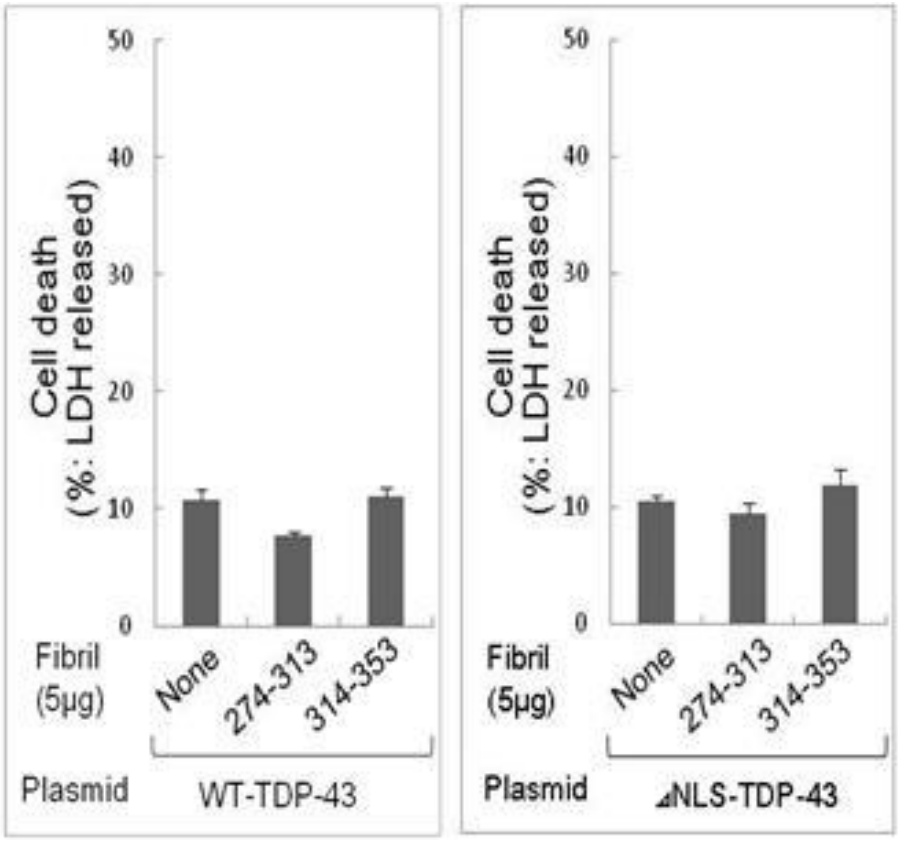
Cell death
(%: LDH released)
50
40
30
20
10
0
Fibril
(5μg)
None
274-313
314-353
Plasmid
WT-TDP-43
Cell death
(%: LDH released)
50
40
30
20
10
0
Fibril
(5μg)
None
274-313
314-353
Plasmid
ΔNLS-TDP-43

Fig. 17

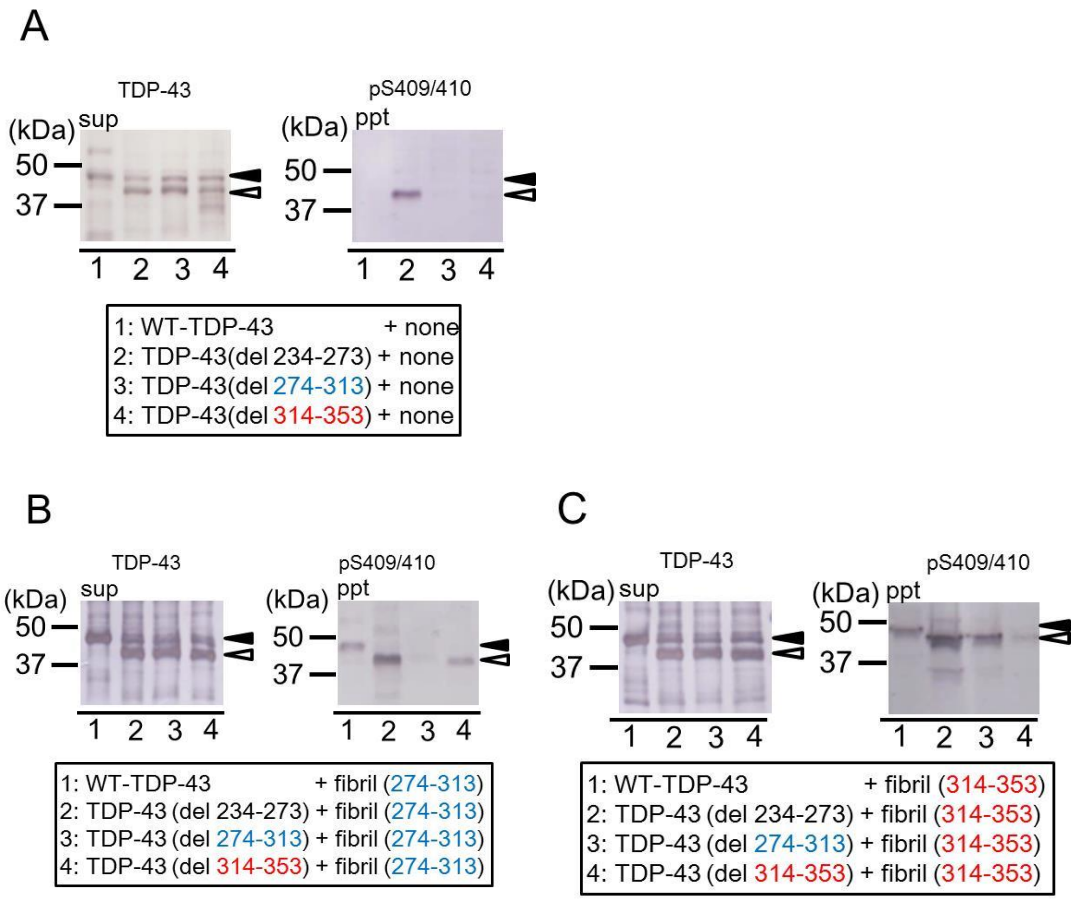
A
TDP-43
sup
(kDa)
50
37
1 2 3 4
pS409/410
ppt
(kDa)
50
37
1 2 3 4
1: WT-TDP-43 + none
2: TDP-43(del 234-273) + none
3: TDP-43(del 274-313) + none
4: TDP-43(del 314-353) + none
B
TDP-43
sup
(kDa)
50
37
1 2 3 4
pS409/410
ppt
(kDa)
50
37
1 2 3 4
1: WT-TDP-43 + fibril (274-313)
2: TDP-43 (del 234-273) + fibril (274-313)
3: TDP-43 (del 274-313) + fibril (274-313)
4: TDP-43 (del 314-353) + fibril (274-313)
C
TDP-43
(kDa) sup
50
37
1 2 3 4
pS409/410
(kDa) ppt
50
37
1 2 3 4
1: WT-TDP-43 + fibril (314-353)
2: TDP-43 (del 234-273) + fibril (314-353)
3: TDP-43 (del 274-313) + fibril (314-353)
4: TDP-43 (del 314-353) + fibril (314-353)

Fig. 18

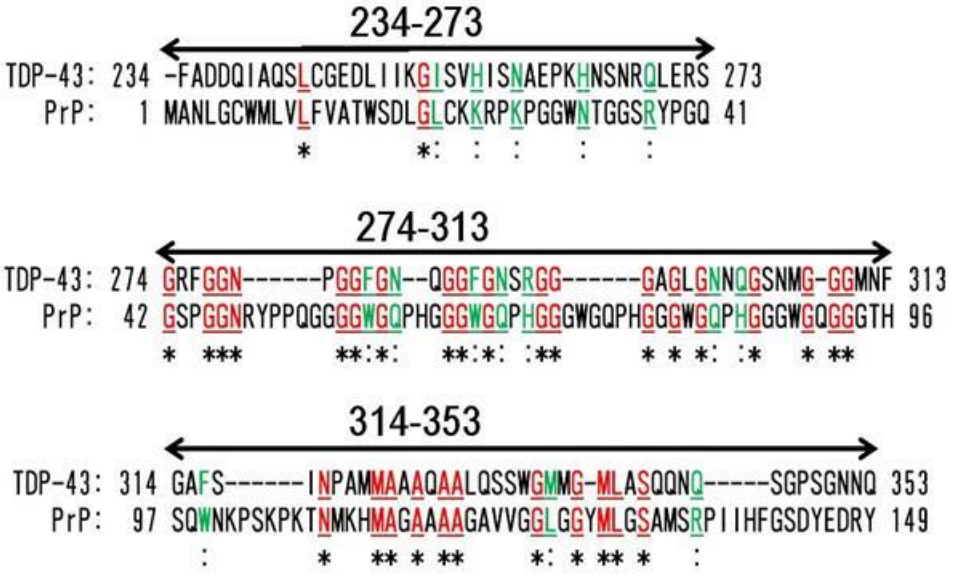
234-273
TDP-43: 234 -FADDQIAQSLCGEDLIIKGISVHISNAEPKHNSNRQLERS 273
PrP: 1 MANLGCWMLVLFVATWSDLGLCKKRPKPGGWNTGGSRYPGQ 41
274-313
TDP-43: 274 GRFGGN------PGGFGN--QGGFGNSRGG------GAGLGNNQGSNMG-GGMNF 313
PrP: 42 GSPGGNRYPPQGGGGWGQPHGGGWGQPHGGGWGQPHGGGWGQPHGGGWGQGGGTH 96
314-353
TDP-43: 314 GAFS------INPAMMAAAQAALQSSWGMMG-MLASQQNQ-----SGPSGNNQ 353
PrP: 97 SQWNKPSKPKTNMKHMAGAAAAGAVVGGLGGYMLGSAMSRPIIHFGSDYEDRY 149

Fig. 19

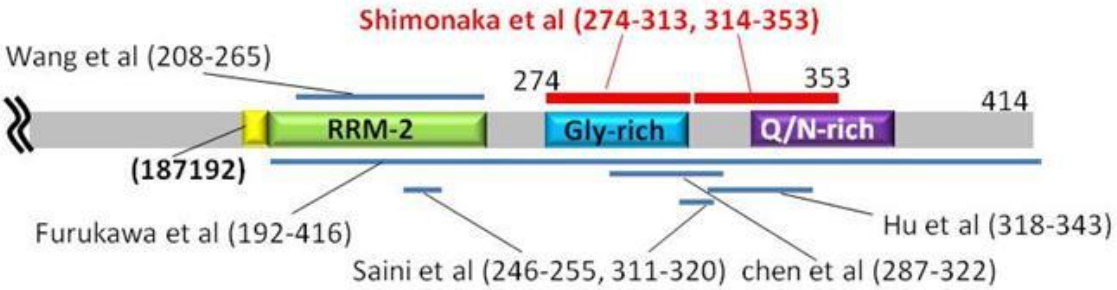
Shimonaka et al (274-313, 314-353)
Wang et al (208-265)
274
353
414
RRM-2
Gly-rich
Q/N-rich
(187192)
Furukawa et al (192-416)
Hu et al (318-343)
Saini et al (246-255, 311-320)
chen et al (287-322)

Fig. 20